Transmit Antenna Subset Selection for Single and Multiuser Spatial Modulation Systems Operating in Frequency Selective Channels

Rakshith Rajashekar, *Senior Member, IEEE*, K.V.S. Hari, *Fellow, IEEE* and L. Hanzo, *Fellow, IEEE*

***Abstract*—The extensive study of transmit antenna (TA) subset selection (TAS) in the context of spatial modulation (SM) has recently revealed that significant performance gains are attainable compared to SM systems operating without TAS. However, the existing TAS techniques conceived for SM were studied by considering a frequency-flat channel, which does not represent practical frequency-selective channels. In this paper, we address this open problem by designing TAS schemes for zero-padded single-carrier SM systems. Specifically, we employ a partial successive interference cancellation (SIC) receiver and invoke Euclidean distance based transmit antenna subset selection (ED-TAS) for each of the sub-channels. Furthermore, we show using theoretical analysis that the parallel sub-channels obtained are nearly identical, which enables us to employ majority logic decision to obtain a single TA subset to be used in all the sub-channels. The computational burden is additionally reduced by restricting the number of sub-channels over which the ED-TAS technique is invoked. Furthermore, the proposed TAS schemes are extended to the multi-user scenario. The theoretical insights developed are validated using simulation results. Specifically, a signal-to-noise ratio (SNR) gain as high as 3dB is observed in the single user scenario and about 1dB in case of a two-user scenario upon employing our TAS.**

***Index Terms*—Antenna subset selection, diversity gain, frequency selective channel, multiuser communication.**

I. Introduction

Spatial modulation (SM) [1]-[12] is a relatively new multiple-input multiple-output (MIMO) scheme that requires a single radio frequency (RF) chain at the transmitter in comparison to the conventional MIMO systems [13], which require multiple RF chains. Specifically, the SM system activates only a single transmit antenna (TA) out of several in each channel use, where the choice of the active TA is made based on the data bits to be transmitted. Furthermore, a symbol selected from a conventional signal set such as QAM/PSK is transmitted over the selected TA. Since only a single TA is activated in each channel use, the SM system completely eliminates the inter-channel interference (ICI) at the receiver, thereby enabling low-complexity single-stream ML detection [9]. The benefits of energy efficient transmitter and of low-complexity optimal detection at the receiver have promoted the SM scheme to an attractive candidate for next generation wireless systems [11], [12].

Although the SM system is capable of giving a better bit error rate (BER) performance [1]-[2] than the conventional MIMO schemes at low and moderate throughputs, it suffers from the lack of transmit diversity gain owing to having a single available RF chain at the transmitter. A significant research effort was invested in improving the transmit diversity gain by employing both open- and closed-loop techniques. The *open-loop techniques* mainly constitute an amalgamation of space-time block coding [14] with the SM scheme. Specifically, an Alamouti code [15] aided SM scheme was conceived in [16], while a complex interleaved orthogonal design was proposed in [17]. As a further development, an SM scheme employing Alamouti STBC having a cyclic structure was proposed in [18], while an SM scheme also relying on Alamouti STBC with temporal permutations was conceived in [19]. All the aforementioned schemes achieve a transmit diversity order of two, while requiring two transmit RF chains, except for the scheme in [17], which requires a single transmit RF chain.

The *closed loop techniques* of [20]-[32] mainly rely on modulation-order selection, antenna-subset selection and transmit precoding (TPC) schemes. Specifically, a link-adaptive modulation scheme was studied in [20], while both capacity based and Euclidean distance (ED) based transmit antenna selection (ED-TAS) schemes were proposed in [21]. Their performances were studied under imperfect channel conditions in [22]. Furthermore, low-complexity antenna selection algorithms were proposed in [23], [24]. The transmit diversity order of ED-TAS was quantified in [25], while Sun *et al.* [26] proposed a cross-entropy based method for reducing the search complexity of ED-TAS. In [27], Yang *et al.* proposed an improved low-complexity implementation of ED-TAS by striking a beneficial performance vs. complexity trade-off. Recently, Sun *et al.* [28] have proposed a reduced-dimensional ED-TAS-equivalent criterion, which results in the same performance as that of ED-TAS, albeit at a reduced complexity. In [29], Naresh *et al.* have studied the ED based mirror activation pattern selection schemes in the context of RF-mirror aided spatial modulation systems. In [30], the authors have proposed a generalized transmit and receive diversity condition for

R. Rajashekar and L. Hanzo are with the School of ECS, University of Southampton, SO17 1BJ, UK (e-mail: R.Mysore-Rajashekar@soton.ac.uk, lh@ecs.soton.ac.uk).

K.V.S. Hari is with the Dept. of ECE, Indian Institute of Science, Bangalore, 560012, India (e-mail: hari@ece.iisc.ernet.in).

The financial support of the EPSRC projects EP/P034284/1, EP/N004558/1 and EP/L018659/1, as well as of the European Research Council's Advanced Fellow Grant under the Beam-Me-Up project and of the Royal Society's Wolfson Research Merit Award is gratefully acknowledged. All data supporting this study are openly available from the University of Southampton repository at http://doi.org/10.5258/SOTON/D0433

TABLE I
SUMMARY OF THE VARIOUS EXISTING CLOSED-LOOP SM TRANSMISSION SCHEMES.

	Contributions
P. Yang *et al.* [20]	Link adaptive SM based on modulation order selection were proposed, where both signal and spatial constellation sizes are chosen based on the channel condition.
R. Rajashekar *et al.* [21], [22]	Capacity optimized and ED-TAS schemes for SM systems were proposed and studied in perfect and imperfect channel estimate conditions.
Z. Zhau *et al.* [23]	Reduced complexity TAS schemes based on pairwise symbol error probability and antenna correlation information were proposed.
N. Wang *et al.* [24]	The computational complexity of ED-TAS was further reduced by exploiting the rotational symmetry in the signal constellation.
R. Rajashekar *et al.* [25]	The achievable transmit diversity order by the ED-TAS was quantified.
Z. Sun *et al.* [26]	The ED-TAS problem was reformulated as a combinatorial optimization problem, which was solved by employing the cross-entropy method.
P. Yang *et al.* [27]	A QR decomposition and error vector magnitude based TAS schemes were proposed as alternate low-complexity solutions to ED-TAS.
Z. Sun *et al.* [28]	Relying on matrix dimension reduction, an ED-TAS-equivalent criterion was developed. The computational complexity of ED-TAS was reduced by tree search and decremental TAS methods.
Y. Naresh *et al.* [29]	Mirror activation pattern selection based on Euclidean distance metric was proposed.
R. Rajashekar *et al.* [30]	A generalized transmit and receive diversity condition is proposed for feedback assisted MIMO systems based on ED metric.
M. C. Lee *et al.* [31]	TPC schemes were conceived for SM systems based on maximizing the minimum ED and minimizing the transmit signal power.
P. Yang *et al.* [32]	TPC schemes based on maximizing the minimum ED and minimizing the upper bound on the BER were proposed.

Note : All the above schemes assume frequency-flat fading scenario.

MIMO systems based on the ED metric. Furthermore, their applications in the context of full-duplex drone communication employing SM was studied. In [31], Lee *et al.* proposed TPC schemes for SM systems based on the ED as well as on signal power metrics, while Yang *et al.* [32] proposed TPC schemes based on maximizing the minimum ED as well as minimizing the BER upper bound.

Table I summarizes the various closed-loop SM transmission schemes discussed so far.

Note that while the SM schemes discussed above correspond to the diversity enhancement methods meant for coherent communication, where the channel state information (CSI) is assumed to be available at the receiver, a significant amount of research effort has also been invested in its non-coherent counterpart [33]. Since this paper mainly deals with coherent SM, we will not delve into the details of non-coherent diversity enhancement techniques conceived for SM [34]-[42].

Against this background, the following are the contributions of this paper:

1) Owing to the high transmit diversity order attainable by ED-TAS [25], it has attracted significant research interests in the recent past. However, all the existing antenna subset selection schemes [21]-[28], including the ED-TAS have only been studied under flat-fading channel conditions, which do not reflect the realistic channel conditions, where the channel is frequency selective. To the best of our knowledge, the antenna subset selection problem in SM systems operating in the frequency selective channel has not been studied in the open literature. Hence we conceive a SM system operating in a frequency selective channel with the aid of zero-padded single carrier (ZP-SC) transmission [6]. Specifically, we employ the partial interference cancellation receiver relying on successive interference cancellation (Partial-SIC) [6] to convert the frequency selective channel into K parallel non-interfering sub-channels and invoke ED-TAS over each of these sub-channels. Since K can be large, the feedback overhead of $K \log_2 \lceil \binom{N_t}{N_{SM}} \rceil_{2^p}$ bits would be very high, where $\lceil \cdot \rceil_{2^p}$ represents the ceiling operator to the nearest integer power of two. Considering the fact that the bandwidth of the feedback channel is limited, it may not be feasible to covey all the $K \log_2 \lceil \binom{N_t}{N_{SM}} \rceil_{2^p}$ bits that encode the antenna subsets to be used at the transmitter. This issue is overcome by employing a *majority* logic based TA subset selection without compromising

the performance, where the TA subset that appears in the majority of the K sub-channels is chosen. This TA selection scheme is termed as the majority logic based TA subset selection (MAJ-TAS). Thanks to the channel symmetry that arises due to Partial-SIC (refer to Proposition 3), more than 90% of the parallel sub-channels are observed to yield the same optimal antenna subset under ED-TAS. Furthermore, owing to having an identical TA subset in a large number of sub-channels, we can further reduce the computational complexity by invoking ED-TAS over only a few sub-channels instead of over all the K sub-channels. The reduced complexity MAJ-TAS scheme, where the ED-TAS is invoked over only $L \ll K$ sub-channels is termed as L-MAJ-TAS.

2) Secondly, we propose a space-division multiple access (SDMA) aided SM system for uplink communication in a frequency selective channel, where we generalise the Partial-SIC decoding conceived for mitigating both the inter-channel and inter-user interference during decoding each user's signal. This decoding algorithm is termed as the multiuser Partial-SIC receiver (MU-SIC). Furthermore, with the aid of MU-SIC we propose a TAS scheme for multiuser SM communication, a problem which has hitherto not been studied in the literature. More specifically, we consider the uplink communication scenario, where the base station (BS) is assumed to have N_r receive antennas with equal number of RF chains and serving U users, each equipped with N_t TAs. Each of the users is assumed to employ only $N_{SM} \leq N_t$ TAs for SM, where the TA subset at each of the users is chosen based on the information fed back from the BS.

The remainder of the paper is organized as follows. The single and multiuser SM systems operating in the frequency selective channel are described in Section II. The proposed single and multiuser TAS algorithms are presented in Section III. Our simulation results are discussed in Section IV, while Section V concludes the paper.

II. System Model

In this section, we briefly describe the single and multiuser SM system models operating with the aid of TAS in a frequency selective channel using the notations in the footnote[1].

[1]*Notations:* $\mathbb{C}$ and $\mathbb{R}$ represent the field of complex and real numbers, respectively. The uppercase boldface letters represent matrices and lowercase boldface letters represent vectors. The notations of $\|\cdot\|_F$ and $\|\cdot\|$ represent the Frobenious norm of a matrix and the two-norm of a vector, respectively. The notations of $(\cdot)^H$ and $(\cdot)^T$ indicate the Hermitian transpose and transpose of a vector/matrix, respectively, while $|\ \cdot\ |$ represents the magnitude of a complex quantity, or the cardinality of a given set. $\mathbf{H}([c:d],:)$ represents a matrix with rows $c, c+1, \ldots, d-1, d$ of $\mathbf{H}$ and $\mathbf{H}(:,[c:d])$ is a matrix with columns $c, c+1, \ldots, d-1, d$ of $\mathbf{H}$. $\mathsf{span}(\mathbf{A})$ represents the space spanned by the columns of $\mathbf{A}$. $\mathsf{Tr}(\cdot)$ represents the trace of a matrix. Given a matrix $\mathbf{A}$, the projection matrix onto its column space is denoted by $\mathsf{Proj}(\mathbf{A})$. Given a set $\mathcal{A}$, $\mathsf{maj}(\mathcal{A})$ represents an element in $\mathcal{A}$ that has the highest number of occurrences compared to any other element in $\mathcal{A}$. Expected value of a random variable Y is denoted by $\mathbb{E}(Y)$. A circularly symmetric complex-valued Gaussian distribution with a mean of μ and a variance of σ^2 is represented by $\mathcal{CN}(\mu, \sigma^2)$.

A. Single User SM System with TAS

Consider a MIMO system having N_r receive as well as N_t TAs, and operating in a quasi-static frequency-selective fading channel having P resolvable paths between each of the transmit and receive antenna pairs. Let the number of antennas used for SM be $N_{SM} \leq N_t$. The received signal vector corresponding to the i^{th} channel use is given by

$$\mathbf{y}_i = \sum_{j=0}^{P-1} \mathbf{H}_j \mathbf{x}_{i-j} + \mathbf{n}_i, \tag{1}$$

where $\mathbf{y}_j \in \mathbb{C}^{N_r \times 1}$ and $\mathbf{x}_j \in \mathbb{C}^{N_t \times 1}$ are the vectors received and transmitted in the j^{th} channel use, $\mathbf{H}_k \in \mathbb{C}^{N_r \times N_t}$ is the k^{th} multipath channel matrix and $\mathbf{n}_j \in \mathbb{C}^{N_r \times 1}$ is the noise vector in the j^{th} channel use. The entries of the multipath channel matrix $\mathbf{H}_k$ are from $\mathcal{CN}(0, \omega_0 \beta^k)$, where we have $0 \leq \beta \leq 1$ and $\sum_{k=0}^{P-1} \omega_0 \beta^k = 1$, and those of the noise vector are from $\mathcal{CN}(0, \sigma^2)$, where σ^2 is the noise variance per complex dimension, which is taken to be $\sigma^2 = \frac{1}{\rho}$ in order to ensure that the average received SNR at each receive antenna is ρ. Furthermore, we assume that $\mathbf{x}_k$ has unity average energy, i.e. the input signal constellation such as PSK/QAM is normalized to have unit energy.

Assuming that each data frame is prefixed with $(P-1)$ zeros and the K transmission symbols constitute a single data frame, the q^{th} zero-padded data frame is given by

$$\left[\underbrace{\mathbf{0}, \mathbf{0}, \ldots, \mathbf{0}}_{P-1 \text{ zero vectors}}, \underbrace{\mathbf{x}_{K(q-1)+1}, \mathbf{x}_{K(q-1)+2}, \ldots, \mathbf{x}_{K(q-1)+K}}_{K \text{ data vectors}} \right],$$

where $\mathbf{0}$ denotes an all-zero vector of size $(N_t \times 1)$. The q^{th} received data frame is given by (2) in the next page, where $K' = K + P - 1$ and $\mathbf{O}$ represents a $(N_r \times N_t)$-element zero matrix. Since the number of paths is P, $(P-1)$-length zero-padding ensures that the successive data frames do not suffer from inter-frame interference. In the SM scheme, each transmitted vector is given by [1]

$$\hat{\mathbf{x}}_k = [\underbrace{0, \ldots, 0}_{l_k - 1}, s_k, \underbrace{0, \ldots, 0}_{N_t - l_k}]^T \in \mathbb{C}^{N_t \times 1}, \tag{3}$$

where s_k is a complex symbol from the signal set $\mathcal{S}$ having $|\mathcal{S}| = M$ and $l_k \in \mathcal{A}_k \subset \mathcal{A} = \{i\}_{i=1}^{N_t}$, where $\mathcal{A}_k$ represents the TA subset chosen for SM in the k^{th} channel use. Thus, each $\mathbf{x}_k$ may assume $N_{SM} M$ different values, since $|\mathcal{A}_k| = N_{SM}$ for $0 \leq k \leq K-1$. The corresponding set of transmit vectors is given by $\mathcal{X}_k = \{\hat{\mathbf{x}}_k \mid l_k \in \mathcal{A}_k, s_k \in \mathcal{S}\}$.

B. Multiuser SM System with TAS

Consider the uplink communication scenario, where the BS is assumed to have N_r receive antennas with equal number of RF chains, and serving U users simultaneously with aid of zero padded single carrier transmissions. Since all the U users are served simultaneously by the BS, each user's signal experiences interference from the other users' signal at the BS. Analogous to (2), the data frame received by the BS is given

$$\underbrace{\begin{bmatrix} \mathbf{y}_{K'(q-1)+1} \\ \mathbf{y}_{K'(q-1)+2} \\ \vdots \\ \mathbf{y}_{K'(q-1)+K'} \end{bmatrix}}_{\hat{\mathbf{y}}} = \underbrace{\begin{bmatrix} \mathbf{H}_0 & \mathbf{O} & \dots & \mathbf{O} & \mathbf{O} \\ \mathbf{H}_1 & \mathbf{H}_0 & \dots & \mathbf{O} & \mathbf{O} \\ \vdots & \vdots & \ddots & \vdots & \vdots \\ \mathbf{H}_{P-1} & \mathbf{H}_{P-2} & \ddots & \mathbf{H}_0 & \mathbf{O} \\ \mathbf{O} & \mathbf{H}_{P-1} & \ddots & \mathbf{H}_1 & \mathbf{H}_0 \\ \vdots & \vdots & \ddots & \vdots & \vdots \\ \mathbf{O} & \mathbf{O} & \dots & \mathbf{H}_{P-1} & \mathbf{H}_{P-2} \\ \mathbf{O} & \mathbf{O} & \dots & \mathbf{O} & \mathbf{H}_{P-1} \end{bmatrix}}_{\hat{\mathbf{H}} \text{ of size } N_r(K+P-1)\times KN_t} \underbrace{\begin{bmatrix} \mathbf{x}_{K(q-1)+1} \\ \mathbf{x}_{K(q-1)+2} \\ \vdots \\ \mathbf{x}_{K(q-1)+K} \end{bmatrix}}_{\hat{\mathbf{x}}} + \underbrace{\begin{bmatrix} \mathbf{n}_{K'(q-1)+1} \\ \mathbf{n}_{K'(q-1)+2} \\ \vdots \\ \mathbf{n}_{K'(q-1)+K'} \end{bmatrix}}_{\hat{\mathbf{n}}}. \quad (2)$$

by

$$\hat{\mathbf{y}} = \sum_{j=1}^{U} \hat{\mathbf{H}}^{(j)} \hat{\mathbf{x}}^{(j)} + \hat{\mathbf{n}}, \quad (4)$$

where $\hat{\mathbf{H}}^{(j)}$ represents the block Toeplitz channel matrix between the BS and the j^{th} user, while $\hat{\mathbf{x}}^{(j)} \in \mathbb{C}^{KN_t}$ is the data stream of the j^{th} user. Analogous to the single-user case, the transmit vector of the j^{th} user is given by

$$\hat{\mathbf{x}}_k^{(j)} = [\underbrace{0, \dots, 0}_{l_k^{(j)}-1}, s_k^{(j)}, \underbrace{0, \dots, 0}_{N_t - l_k^{(j)}}]^T \in \mathbb{C}^{N_t \times 1}, \quad (5)$$

where $s_k^{(j)}$ is the j^{th} user's complex symbol chosen from the signal set $\mathcal{S}$ and $l_k^{(j)} \in \mathcal{A}_k^{(j)} \subset \mathcal{A} = \{i\}_{i=1}^{N_t}$, where $\mathcal{A}_k^{(j)}$ represents the j^{th} user's TA subset chosen for SM in the k^{th} channel use. The j^{th} user's set of transmit vectors for the k^{th} channel use is given by $\mathcal{X}_k^{(j)} = \{\hat{\mathbf{x}}_k^{(j)} \mid l_k^{(j)} \in \mathcal{A}_k, s_k^{(j)} \in \mathcal{S}\}$.

III. Proposed TAS Algorithms for SM system in Frequency Selective channel

In this section, we present various TAS algorithms proposed for an SM system operating in the frequency selective channel.

A. Proposed Partial-SIC aided TAS (SIC-TAS) Algorithm

We first convert the system in (2) into a set of non-interfering parallel channels by employing partial interference cancellation receiver (PIC-R) [6], whose details are given as follows. Let

$$\mathcal{I}_i = \{N_t i + 1, N_t i + 2, \dots, N_t(i+1)\}, \quad (6)$$

for $i = 0, 1, \cdots, K-1$, such that $\cup_{i=0}^{K-1} \mathcal{I}_i = \mathcal{I} = \{i\}_{i=1}^{N_t K}$ and $\mathbf{G}_{\mathcal{I}_i}$ be the matrix having columns of $\hat{\mathbf{H}}$ that are indexed by the elements of $\mathcal{I}_i$. The system in (2) can be written as

$$\hat{\mathbf{y}} = \sum_{i=0}^{K-1} \mathbf{G}_{\mathcal{I}_i} \hat{\mathbf{x}}_i + \hat{\mathbf{n}}, \quad (7)$$

where $\hat{\mathbf{x}}_i = \hat{\mathbf{x}}([iN_t+1 : (i+1)N_t]) \in \mathbb{C}^{N_t}$, for $0 \le i \le K-1$.

Let $\mathbf{G}_{\mathcal{I}_k}^c = \left[\mathbf{G}_{\mathcal{I}_0}, \mathbf{G}_{\mathcal{I}_1}, \dots, \mathbf{G}_{\mathcal{I}_{k-1}}, \mathbf{G}_{\mathcal{I}_{k+1}}, \dots, \mathbf{G}_{\mathcal{I}_{K-1}}\right]$. The matrix projecting on to the orthogonal complement space of $\mathbf{G}_{\mathcal{I}_k}^c$ is given by $\mathbf{P}_{\mathcal{I}_k} = \mathbf{I}_{N_r(K+P-1)} - \mathbf{Q}_{\mathcal{I}_k}$, where $\mathbf{Q}_{\mathcal{I}_k} = \mathbf{G}_{\mathcal{I}_k}^c \left((\mathbf{G}_{\mathcal{I}_k}^c)^H \mathbf{G}_{\mathcal{I}_k}^c\right)^{-1} (\mathbf{G}_{\mathcal{I}_k}^c)^H$. Thus, we have $\mathbf{P}_{\mathcal{I}_k} \mathbf{G}_{\mathcal{I}_i} = \mathbf{0}$ for $i \in \{j\}_{j=0}^{K-1} \setminus k$. Consider $\mathbf{z}_{\mathcal{I}_k} = \mathbf{P}_{\mathcal{I}_k} \hat{\mathbf{y}}$ given by

$$\mathbf{z}_{\mathcal{I}_k} = \mathbf{P}_{\mathcal{I}_k} \sum_{i=1}^{K-1} \mathbf{G}_{\mathcal{I}_i} \hat{\mathbf{x}}_i + \mathbf{P}_{\mathcal{I}_k} \hat{\mathbf{n}}, \quad (8)$$

$$= \mathbf{P}_{\mathcal{I}_k} \mathbf{G}_{\mathcal{I}_k} \hat{\mathbf{x}}_k + \mathbf{P}_{\mathcal{I}_k} \hat{\mathbf{n}}. \quad (9)$$

The PIC-R solution for the k^{th} subsystem is given by

$$(\hat{\mathbf{x}}_k)_{PIC-R} = \arg \min_{\mathbf{x} \in \mathcal{X}_k} \|\mathbf{z}_{\mathcal{I}_k} - \mathbf{P}_{\mathcal{I}_k} \mathbf{G}_{\mathcal{I}_k} \mathbf{x}\|^2, \quad (10)$$

for $0 \le k \le K-1$, where $\mathcal{X}_k$ represents the set of transmit vectors chosen for the k^{th} channel use depending on $\mathcal{A}_k$.

Proposition 1: The PIC-R solution in (10) achieves a diversity gain of $N_r P(N_t - N_{SM} + 1)$ when $\mathcal{X}_k$, $0 \le k \le K-1$ are chosen based on ED-TAS [21].

Proof: The proof directly follows from Proposition 3 [6] and Proposition 2 [25]. ■

The ED-TAS [25] based TA subset is given by

$$\mathcal{A}_k = \arg \max_{\substack{\mathcal{A}' \subset \mathcal{A}, \\ |\mathcal{A}'| = N_{SM}}} \min_{\mathbf{x}_1 \neq \mathbf{x}_2} \|\mathbf{R}_k(:, \mathcal{A}')(\mathbf{x}_1 - \mathbf{x}_2)\|^2, \quad (11)$$

where $\mathbf{R}_k = \mathbf{P}_{\mathcal{I}_k} \mathbf{G}_{\mathcal{I}_k}$, $\mathbf{x}_1$ and $\mathbf{x}_2$ are $N_{SM} \times 1$ SM vectors, whose non-zero elements are drawn from $\mathcal{S}$. Note that although Proposition 1 guarantees a high transmit diversity gain, the overhead involved in computing the optimal antenna subsets (11) and conveying that information to the transmitter is potentially enormous. Specifically, we have the following major issues, when invoking ED-TAS over all the K sub-channels.

- Since ED-TAS is invoked over each of the K sub-channels, the K antenna subsets require $K \log_2(\lceil \binom{N_t}{N_{SM}} \rceil_{2^p})$ bits for conveying the chosen antenna subsets over the feedback channel to the transmitter. This may impose a significant overhead on the feedback channel, which has a limited bandwidth;
- Secondly, the computational complexity involved in employing ED-TAS over each of the sub-channels may become excessive when K is very large.

The above issues can be overcome by the proposed SIC-TAS algorithm (Algorithm 1), which employs Partial-SIC [6] instead of PIC-R.

Note that the matrix computations in Step 1 of Algorithm 1 can be significantly reduced by employing the results from

Algorithm 1 SIC-TAS for the ZP-SC SM system

Require: $k=0$, $\mathcal{A}_{SIC}=\{\cdot\}$.
while $k<K$ **do**
1. $\mathbf{G}^c_{\mathcal{I}_k}=\left[\mathbf{G}_{\mathcal{I}_{k+1}},\ldots,\mathbf{G}_{\mathcal{I}_{K-1}}\right]$,
$\mathbf{Q}_{\mathcal{I}_k}=\mathbf{G}^c_{\mathcal{I}_k}\left((\mathbf{G}^c_{\mathcal{I}_k})^H\mathbf{G}^c_{\mathcal{I}_k}\right)^{-1}(\mathbf{G}^c_{\mathcal{I}_k})^H$,
$\mathbf{P}_{\mathcal{I}_k}=\mathbf{I}_{N_r(K+P-1)}-\mathbf{Q}_{\mathcal{I}_k}$,
$\mathbf{R}_k=\mathbf{P}_{\mathcal{I}_k}\mathbf{G}_{\mathcal{I}_k}$.
2. Obtain

$$\mathcal{A}_k=\arg\max_{\substack{\mathcal{A}'\subset\mathcal{A},\\ |\mathcal{A}'|=N_{SM}}}\min_{\mathbf{x}_1\neq\mathbf{x}_2}\|\mathbf{R}_k(:,\mathcal{A}')(\mathbf{x}_1-\mathbf{x}_2)\|^2,$$

$\mathcal{A}_{SIC}\leftarrow\mathcal{A}_{SIC}\cup\mathcal{A}_k$,
$k\leftarrow k+1$.
end while
return $\mathcal{A}_{SIC}$

[43]. However, the computational complexity involved in Step 2 is quite high, even when considering the latest low-complexity ED-TAS solutions of [28]. In order to reduce the computational burden involved in Step 2, it is important to develop insight into the set of antenna subsets $\mathcal{A}_{SIC}$.

Note that in case of Partial-SIC, the transmit vectors are decoded and cancelled from the received signal in the order $\hat{\mathbf{x}}_0,\hat{\mathbf{x}}_1,\ldots,\hat{\mathbf{x}}_{K-1}$ by taking $\mathbf{G}^c_{\mathcal{I}_k}=\left[\mathbf{G}_{\mathcal{I}_{k+1}},\ldots,\mathbf{G}_{\mathcal{I}_{K-1}}\right]$ for $0\leq k\leq K-1$. In order to gain insight into the nature of the parallel sub-channels in Partial-SIC, let us partition $\mathbf{G}^c_{\mathcal{I}_k}$ into $[\mathbf{J}_k,\mathbf{W}_k]$, where $\mathbf{J}_k=\left[\mathbf{G}_{\mathcal{I}_{k+1}},\ldots,\mathbf{G}_{\mathcal{I}_{k+P-1}}\right]$ corresponds to the sub-channels that interfere with $\mathbf{G}_{\mathcal{I}_k}$ and $\mathbf{W}_k=\left[\mathbf{G}_{\mathcal{I}_{k+P}},\ldots,\mathbf{G}_{\mathcal{I}_{K-1}}\right]$ corresponds to the sub-channels that are orthogonal to $\mathbf{G}_{\mathcal{I}_k}$. The following proposition throws light on the interfering and non-interfering sub-channels in Partial-SIC.

Proposition 2: In the Partial-SIC detection using the decoding order mentioned above, each of the parallel sub-channels obeys:

$$\mathbf{P}_{\mathcal{I}_k}\mathbf{G}_{\mathcal{I}_k}\equiv[\mathbf{I}_{N_r(K+P-1)}-\mathsf{Proj}(\mathbf{P}_{\mathcal{I}_{k+P-1}}\mathbf{J}_k)]\mathbf{G}_{\mathcal{I}_k}. \quad (12)$$

Proof: Recall that $\mathbf{P}_{\mathcal{I}_k}=\mathbf{I}_{N_r(K+P-1)}-\mathbf{Q}_{\mathcal{I}_k}$, where $\mathbf{Q}_{\mathcal{I}_k}=\mathbf{G}^c_{\mathcal{I}_k}\left((\mathbf{G}^c_{\mathcal{I}_k})^H\mathbf{G}^c_{\mathcal{I}_k}\right)^{-1}(\mathbf{G}^c_{\mathcal{I}_k})^H$. Since $\mathbf{G}^c_{\mathcal{I}_k}$ can be partitioned as $[\mathbf{J}_k,\mathbf{W}_k]$, we have

$$\mathbf{Q}_{\mathcal{I}_k}=[\mathbf{J}_k,\mathbf{W}_k]\begin{bmatrix}\mathbf{J}_k^H\mathbf{J}_k & \mathbf{J}_k^H\mathbf{W}_k\\ \mathbf{W}_k^H\mathbf{J}_k & \mathbf{W}_k^H\mathbf{W}_k\end{bmatrix}^{-1}\begin{bmatrix}\mathbf{J}_k^H\\ \mathbf{W}_k^H\end{bmatrix}. \quad (13)$$

By invoking the block matrix inversion of [44], we have

$$\begin{bmatrix}\mathbf{J}_k^H\mathbf{J}_k & \mathbf{J}_k^H\mathbf{W}_k\\ \mathbf{W}_k^H\mathbf{J}_k & \mathbf{W}_k^H\mathbf{W}_k\end{bmatrix}^{-1}=\begin{bmatrix}\mathbf{A} & \mathbf{B}\\ \mathbf{C} & \mathbf{D}\end{bmatrix}, \quad (14)$$

where $\mathbf{A}$, $\mathbf{B}$, $\mathbf{C}$ and $\mathbf{D}$ are given by (15)-(18) in the next page.

Since the columns of $\mathbf{G}_{\mathcal{I}_k}$ are orthogonal to those of $\mathbf{W}_k$, we have

$$\mathbf{Q}_{\mathcal{I}_k}\mathbf{G}_{\mathcal{I}_k}=[\mathbf{J}_k,\mathbf{W}_k]\begin{bmatrix}\mathbf{A} & \mathbf{B}\\ \mathbf{C} & \mathbf{D}\end{bmatrix}\begin{bmatrix}\mathbf{J}_k^H\mathbf{G}_{\mathcal{I}_k}\\ \mathbf{W}_k^H\mathbf{G}_{\mathcal{I}_k}\end{bmatrix}, \quad (19)$$

$$=[\mathbf{J}_k,\mathbf{W}_k]\begin{bmatrix}\mathbf{A} & \mathbf{B}\\ \mathbf{C} & \mathbf{D}\end{bmatrix}\begin{bmatrix}\mathbf{J}_k^H\mathbf{G}_{\mathcal{I}_k}\\ \mathbf{O}\end{bmatrix}, \quad (20)$$

$$=\mathbf{J}_k\mathbf{A}\mathbf{J}_k^H\mathbf{G}_{\mathcal{I}_k}+\mathbf{W}_k\mathbf{C}\mathbf{J}_k^H\mathbf{G}_{\mathcal{I}_k}, \quad (21)$$

$$=\mathbf{J}_k\mathbf{A}\mathbf{J}_k^H\mathbf{G}_{\mathcal{I}_k}-\mathbf{W}_k(\mathbf{W}_k^H\mathbf{W}_k)^{-1}\mathbf{W}_k^H\mathbf{J}_k\mathbf{A}\mathbf{J}_k^H\mathbf{G}_{\mathcal{I}_k}, \quad (22)$$

$$=\left[\mathbf{I}-\mathbf{W}_k(\mathbf{W}_k^H\mathbf{W}_k)^{-1}\mathbf{W}_k^H\right]\mathbf{J}_k\mathbf{A}\mathbf{J}_k^H\mathbf{G}_{\mathcal{I}_k}, \quad (23)$$

$$=\mathbf{P}_{\mathcal{I}_{k+P-1}}\mathbf{J}_k\mathbf{A}\mathbf{J}_k^H\mathbf{G}_{\mathcal{I}_k}. \quad (24)$$

Furthermore, we have

$$\mathbf{A}=\left[\mathbf{J}_k^H\mathbf{J}_k-\mathbf{J}_k^H\mathbf{W}_k(\mathbf{W}_k^H\mathbf{W}_k)^{-1}\mathbf{W}_k^H\mathbf{J}_k\right]^{-1}, \quad (25)$$

$$=\left[\mathbf{J}_k^H(\mathbf{I}-\mathbf{W}_k(\mathbf{W}_k^H\mathbf{W}_k)^{-1}\mathbf{W}_k^H)\mathbf{J}_k\right]^{-1}, \quad (26)$$

$$=\left[\mathbf{J}_k^H\mathbf{P}_{\mathcal{I}_{k+P-1}}\mathbf{J}_k\right]^{-1}. \quad (27)$$

Substituting (27) into (24), we have

$$\mathbf{Q}_{\mathcal{I}_k}\mathbf{G}_{\mathcal{I}_k}=\mathbf{P}_{\mathcal{I}_{k+P-1}}\mathbf{J}_k\left[\mathbf{J}_k^H\mathbf{P}_{\mathcal{I}_{k+P-1}}\mathbf{J}_k\right]^{-1}\mathbf{J}_k^H\mathbf{G}_{\mathcal{I}_k}, \quad (28)$$

$$=\mathsf{Proj}(\mathbf{P}_{\mathcal{I}_{k+P-1}}\mathbf{J}_k)\mathbf{G}_{\mathcal{I}_k}, \quad (29)$$

where we have used the following facts:

i $\mathbf{G}_{\mathcal{I}_k}=\mathbf{P}_{\mathcal{I}_{k+P-1}}\mathbf{G}_{\mathcal{I}_k}$,
ii $\mathbf{P}_{\mathcal{I}_{k+P-1}}=\mathbf{P}^2_{\mathcal{I}_{k+P-1}}$,
iii $\mathbf{P}^H_{\mathcal{I}_{k+P-1}}=\mathbf{P}_{\mathcal{I}_{k+P-1}}$.

(i) follows from the fact that the columns of $\mathbf{G}_{\mathcal{I}_k}$ are orthogonal to those of $\mathbf{W}_k$. Furthermore, (ii) and (iii) follow from the fact that $\mathbf{P}_{\mathcal{I}_{k+P-1}}$ is a projection matrix.

Thus, we have

$$\mathbf{P}_{\mathcal{I}_k}\mathbf{G}_{\mathcal{I}_k}=\mathbf{G}_{\mathcal{I}_k}-\mathbf{Q}_{\mathcal{I}_k}\mathbf{G}_{\mathcal{I}_k}, \quad (30)$$

$$=[\mathbf{I}_{N_r(K+P-1)}-\mathsf{Proj}(\mathbf{P}_{\mathcal{I}_{k+P-1}}\mathbf{J}_k)]\mathbf{G}_{\mathcal{I}_k}. \quad (31)$$

This concludes the proof. ■

From Proposition 2, we have $\mathbf{P}_{\mathcal{I}_k}\mathbf{G}_{\mathcal{I}_k}=[\mathbf{I}_{N_r(K+P-1)}-\mathsf{Proj}(\mathbf{P}_{\mathcal{I}_{k+P-1}}\mathbf{J}_k)]\mathbf{G}_{\mathcal{I}_k}$. A physical interpretation of this equation is that the projection of $\mathbf{G}_{\mathcal{I}_k}$ onto the space, which is orthogonal to $\mathbf{Q}_{\mathcal{I}_k}$ is the same as projecting it onto the space that is orthogonal to its interference space, i.e. to $\mathbf{P}_{\mathcal{I}_{k+P-1}}\mathbf{J}_k$. Note that although the sub-channels in $\mathbf{J}_k$ interfere with $\mathbf{G}_{\mathcal{I}_k}$, only those components of $\mathbf{J}_k$ interfere that are orthogonal to $\mathbf{W}_k$, i.e. $\mathbf{P}_{\mathcal{I}_{k+P-1}}\mathbf{J}_k$. This is so, since the components of $\mathbf{J}_k$ that belong to the space spanned by $\mathbf{W}_k$ do not interfere with $\mathbf{G}_{\mathcal{I}_k}$.

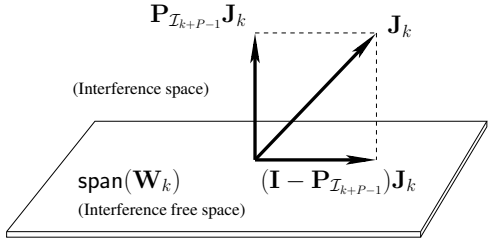

Fig. 1. Pictorial depiction of the components of $\mathbf{J}_k$ that interfere with $\mathbf{G}_{\mathcal{I}_k}$ and that which does not.

$$\mathbf{A} = \left[\mathbf{J}_k^H\mathbf{J}_k - \mathbf{J}_k^H\mathbf{W}_k(\mathbf{W}_k^H\mathbf{W}_k)^{-1}\mathbf{W}_k^H\mathbf{J}_k\right]^{-1}, \tag{15}$$

$$\mathbf{B} = -\left[\mathbf{J}_k^H\mathbf{J}_k - \mathbf{J}_k^H\mathbf{W}_k(\mathbf{W}_k^H\mathbf{W}_k)^{-1}\mathbf{W}_k^H\mathbf{J}_k\right]^{-1}\mathbf{J}_k^H\mathbf{W}_k(\mathbf{W}_k^H\mathbf{W}_k)^{-1}, \tag{16}$$

$$\mathbf{C} = -(\mathbf{W}_k^H\mathbf{W}_k)^{-1}\mathbf{W}_k^H\mathbf{J}_k\left[\mathbf{J}_k^H\mathbf{J}_k - \mathbf{J}_k^H\mathbf{W}_k(\mathbf{W}_k^H\mathbf{W}_k)^{-1}\mathbf{W}_k^H\mathbf{J}_k\right]^{-1}, \tag{17}$$

$$\mathbf{D} = (\mathbf{W}_k^H\mathbf{W}_k)^{-1} + (\mathbf{W}_k^H\mathbf{W}_k)^{-1}\mathbf{W}_k^H\mathbf{J}_k(\mathbf{J}_k^H\mathbf{J}_k - \mathbf{J}_k^H\mathbf{W}_k(\mathbf{W}_k^H\mathbf{W}_k)^{-1}\mathbf{W}_k^H\mathbf{J}_k)^{-1}\mathbf{J}_k^H\mathbf{W}_k(\mathbf{W}_k^H\mathbf{W}_k)^{-1}. \tag{18}$$

A pictorial portrayal of the interfering and non-interfering subspaces is given in Fig. 1. Note that when $P = 1$, then none of the parallel sub-channels experiences any interference. As a result, $\mathcal{A}_{SIC}$ will have a single distinct element. However, in the presence of interference, where $P > 1$, it is not clear whether $\mathcal{A}_{SIC}$ has a single or several distinct elements. The following discussion casts light on this scenario.

Let us now study the variation in sub-channels by considering $\mathbf{P}_{\mathcal{I}_k}\mathbf{G}_{\mathcal{I}_k} = [\mathbf{I}_{N_r(K+P-1)} - \mathsf{Proj}(\mathbf{P}_{\mathcal{I}_{k+P-1}}\mathbf{J}_k)]\mathbf{G}_{\mathcal{I}_k}$ and $\mathbf{P}_{\mathcal{I}_{k+1}}\mathbf{G}_{\mathcal{I}_{k+1}} = [\mathbf{I}_{N_r(K+P-1)} - \mathsf{Proj}(\mathbf{P}_{\mathcal{I}_{k+P}}\mathbf{J}_{k+1})]\mathbf{G}_{\mathcal{I}_{k+1}}$. Before proceeding further, let us define the following matrices:

$$\mathbf{E} = \begin{bmatrix} 0 & 0 & \cdots & 0 & 0 \\ 1 & 0 & \cdots & 0 & 0 \\ 0 & 1 & \cdots & 0 & 0 \\ \vdots & \vdots & \ddots & \vdots & \vdots \\ 0 & 0 & \cdots & 1 & 0 \end{bmatrix} \in \mathbb{R}^{K+P-1 \times K+P-1} \tag{32}$$

and $\mathbf{M} = \mathbf{E} \otimes \mathbf{I}_{N_r}$. Note that the interfering sub-channels in case of $\mathbf{P}_{\mathcal{I}_{k+1}}\mathbf{G}_{\mathcal{I}_{k+1}}$ i.e. $\mathbf{J}_{k+1}$ are constituted by a shifted version of $\mathbf{J}_k$, yielding $\mathbf{M}\mathbf{J}_k = \mathbf{J}_{k+1}$ for $k \leq K - P + 1$. A similar statement holds with regard to $\mathbf{P}_{\mathcal{I}_{k+P-1}}$ and $\mathbf{P}_{\mathcal{I}_{k+P}}$, when K is large. The following proposition exploits these facts to show that the parallel sub-channels in Partial-SIC are essentially the same, except for the shift, when K is large.

Proposition 3: In the Partial-SIC detection associated with the decoding order mentioned earlier, we have

$$\lim_{K\to\infty}(\mathbf{P}_{\mathcal{I}_k}\mathbf{G}_{\mathcal{I}_k} - \mathbf{M}^T\mathbf{P}_{\mathcal{I}_{k+1}}\mathbf{G}_{\mathcal{I}_{k+1}}) = \mathbf{O}. \tag{33}$$

Proof: Since $\mathbf{M}\mathbf{G}_{\mathcal{I}_k} = \mathbf{G}_{\mathcal{I}_{k+1}}$, we have

$$\Delta_k = \mathbf{P}_{\mathcal{I}_k}\mathbf{G}_{\mathcal{I}_k} - \mathbf{M}^T\mathbf{P}_{\mathcal{I}_{k+1}}\mathbf{G}_{\mathcal{I}_{k+1}}, \tag{34}$$

$$= \mathbf{P}_{\mathcal{I}_k}\mathbf{G}_{\mathcal{I}_k} - \mathbf{M}^T\mathbf{P}_{\mathcal{I}_{k+1}}\mathbf{M}\mathbf{G}_{\mathcal{I}_k}, \tag{35}$$

$$= (\mathbf{P}_{\mathcal{I}_k} - \mathbf{M}^T\mathbf{P}_{\mathcal{I}_{k+1}}\mathbf{M})\mathbf{G}_{\mathcal{I}_k}. \tag{36}$$

Furthermore, we have

$$\mathbf{P}_{\mathcal{I}_k} - \mathbf{M}^T\mathbf{P}_{\mathcal{I}_{k+1}}\mathbf{M} = (\mathbf{I} - \mathbf{M}^T\mathbf{M}) + (\mathbf{M}^T\mathbf{Q}_{\mathcal{I}_{k+1}}\mathbf{M} - \mathbf{Q}_{\mathcal{I}_k}). \tag{37}$$

Since $\mathbf{M}^T\mathbf{M} \to \mathbf{I}$ and $\mathbf{M}^T\mathbf{G}^c_{\mathcal{I}_{k+1}} \to \mathbf{G}^c_{\mathcal{I}_k}$ as $K \to \infty$, we have $(\mathbf{P}_{\mathcal{I}_k} - \mathbf{M}^T\mathbf{P}_{\mathcal{I}_{k+1}}\mathbf{M}) \to \mathbf{O}$. This concludes the proof. ■

Remark 1: Note that the results in Proposition 2 and Proposition 3 have wider implications in the context of ZP-SC transmission. Specifically, the equivalence of sub-channels enables various techniques such as (i) beamforming/precoding, (ii) power allocation, (iii) transmit antenna selection, etc. to be invoked at a very low feedback overhead. Explicitly, the above results allow the optimal solutions conceived for one of the subchannels to be used across all the subchannels, when K is sufficiently high. Note that these results are independent of the type of the modulation employed and hence are not restricted to SM. The following corollary consolidates these facts.

Corollary 1: If $\mathbf{S}_k \in \mathbb{C}^{N_t \times N_t}$ and $\mathbf{D}_k \in \mathbb{R}^{N_t \times N_t}$ are the precoding and power allocation matrices associated with $\hat{\mathbf{x}}_k$ in (7), where $\mathbf{S}_k$ is the right singular matrix of $\mathbf{P}_{\mathcal{I}_k}\mathbf{G}_{\mathcal{I}_k}$ and $\mathbf{D}_k$ is the associated water-filling solution [45], then we have $\lim_{K\to\infty}(\mathbf{S}_k - \mathbf{S}_{k+1}) = \mathbf{O}$ and $\lim_{K\to\infty}(\mathbf{D}_k - \mathbf{D}_{k+1}) = \mathbf{O}$.

Proof: If $\mathbf{P}_{\mathcal{I}_k}\mathbf{G}_{\mathcal{I}_k} = \mathbf{U}\mathbf{\Sigma}\mathbf{V}^H$, then we have $\mathbf{P}_{\mathcal{I}_k}\mathbf{G}_{\mathcal{I}_k} = \mathbf{M}^T\mathbf{P}_{\mathcal{I}_{k+1}}\mathbf{G}_{\mathcal{I}_{k+1}}$ from Proposition 3. Thus, we have $\mathbf{P}_{\mathcal{I}_{k+1}}\mathbf{G}_{\mathcal{I}_{k+1}} = \mathbf{M}\mathbf{U}\mathbf{\Sigma}\mathbf{V}^H \equiv \mathbf{U}'\mathbf{\Sigma}\mathbf{V}^H$. Thus, it is evident that the right singular matrix and the singular values of $\mathbf{P}_{\mathcal{I}_k}\mathbf{G}_{\mathcal{I}_k}$ and $\mathbf{P}_{\mathcal{I}_{k+1}}\mathbf{G}_{\mathcal{I}_{k+1}}$ are essentially the same, when $K \to \infty$. Thus, we have $\lim_{K\to\infty}(\mathbf{S}_k - \mathbf{S}_{k+1}) = \mathbf{O}$ and $\lim_{K\to\infty}(\mathbf{D}_k - \mathbf{D}_{k+1}) = \mathbf{O}$. This concludes the proof. ■

In Proposition 3, we have shown that $\lim_{K\to\infty}(\mathbf{P}_{\mathcal{I}_k}\mathbf{G}_{\mathcal{I}_k} - \mathbf{M}^T\mathbf{P}_{\mathcal{I}_{k+1}}\mathbf{G}_{\mathcal{I}_{k+1}}) = \mathbf{O}$. We now develop further insight into $\mathbf{P}_{\mathcal{I}_k}\mathbf{G}_{\mathcal{I}_k} - \mathbf{M}^T\mathbf{P}_{\mathcal{I}_{k+1}}\mathbf{G}_{\mathcal{I}_{k+1}}$ by considering a finite K. We have $\mathbf{M}^T\mathbf{M} = (\mathbf{E} \otimes \mathbf{I}_{N_r})^T(\mathbf{E} \otimes \mathbf{I}_{N_r}) = \mathbf{E}^T\mathbf{E} \otimes \mathbf{I}_{N_r} = \mathsf{diag}(\mathbf{I}_{N_r}, \mathbf{I}_{N_r}, \ldots, \mathbf{I}_{N_r}, \mathbf{O})$. Thus, we have $(\mathbf{I} - \mathbf{M}^T\mathbf{M}) = \mathsf{diag}(\mathbf{O}, \mathbf{O}, \ldots, \mathbf{O}, \mathbf{I}_{N_r})$. Let us now consider $(\mathbf{M}^T\mathbf{Q}_{\mathcal{I}_{k+1}}\mathbf{M} - \mathbf{Q}_{\mathcal{I}_k})$, by restricting $k < K - P - 1$. From Proposition 2, we have

$$\mathbf{Q}_{\mathcal{I}_k} = \mathsf{Proj}(\mathbf{P}_{\mathcal{I}_{k+P-1}}\mathbf{J}_k), \tag{38}$$

$$= \mathbf{P}_{\mathcal{I}_{k+P-1}}\mathbf{J}_k\left[\mathbf{J}_k^H\mathbf{P}_{\mathcal{I}_{k+P-1}}\mathbf{J}_k\right]^{-1}\mathbf{J}_k^H\mathbf{P}_{\mathcal{I}_{k+P-1}}, \tag{39}$$

$$\mathbf{Q}_{\mathcal{I}_{k+1}} = \mathsf{Proj}(\mathbf{P}_{\mathcal{I}_{k+P}}\mathbf{J}_{k+1}), \tag{40}$$

$$= \mathbf{P}_{\mathcal{I}_{k+P}}\mathbf{J}_{k+1}\left[\mathbf{J}_{k+1}^H\mathbf{P}_{\mathcal{I}_{k+P}}\mathbf{J}_{k+1}\right]^{-1}\mathbf{J}_{k+1}^H\mathbf{P}_{\mathcal{I}_{k+P}}. \tag{41}$$

Since $\mathbf{M}\mathbf{J}_{k+1} = \mathbf{J}_k$ when $k < K - P - 1$, we have

$$\mathbf{M}^T\mathbf{Q}_{\mathcal{I}_{k+1}}\mathbf{M} = (\mathbf{M}^T\mathbf{P}_{\mathcal{I}_{k+P}}\mathbf{M})\mathbf{J}_k\left[\mathbf{J}_k^H(\mathbf{M}^T\mathbf{P}_{\mathcal{I}_{k+P}}\mathbf{M})\mathbf{J}_k\right]^{-1} \times \mathbf{J}_k^H(\mathbf{M}^T\mathbf{P}_{\mathcal{I}_{k+P}}\mathbf{M}). \tag{42}$$

It is evident from (40) and (43) that the similarity between $\mathbf{Q}_{\mathcal{I}_k}$ and $\mathbf{M}^T\mathbf{Q}_{\mathcal{I}_{k+1}}\mathbf{M}$ mainly depends on the similarity between $\mathbf{P}_{\mathcal{I}_{k+P-1}}$ and $\mathbf{M}^T\mathbf{P}_{\mathcal{I}_{k+P}}\mathbf{M}$. Furthermore, we have

$$\mathbf{M}^T\mathbf{P}_{\mathcal{I}_{k+P}}\mathbf{M} = \mathbf{M}^T\mathbf{M} - \mathbf{M}^T\mathbf{W}_{k+1}(\mathbf{W}_{k+1}^H\mathbf{W}_{k+1})^{-1}\mathbf{W}_{k+1}^H\mathbf{M}, \tag{43}$$

$$= \mathbf{M}^T\mathbf{M} - \mathbf{M}^T\mathbf{W}_{k+1}(\mathbf{W}_{k+1}^H\mathbf{M}\mathbf{M}^T\mathbf{W}_{k+1})^{-1} \times \mathbf{W}_{k+1}^H\mathbf{M}. \tag{44}$$

Furthermore, it can be shown (refer to Appendix A) that

$$\mathbf{P}_{\mathcal{I}_{k+P-1}} = \mathbf{I} - \mathbf{P}_{\mathcal{I}_{K-2}}\mathbf{M}^T\mathbf{W}_{k+1}(\mathbf{W}_{k+1}^H\mathbf{M}\mathbf{P}_{\mathcal{I}_{K-2}}\mathbf{M}^T\mathbf{W}_{k+1})^- \times \mathbf{W}_{k+1}^H\mathbf{M}. \quad (45)$$

Comparing (45) to (44), we can see that $\mathbf{P}_{\mathcal{I}_{K-2}}\mathbf{M}^T\mathbf{W}_{k+1}$ determines the grade of similarity between $\mathbf{P}_{\mathcal{I}_{k+P-1}}$ and $\mathbf{M}^T\mathbf{P}_{\mathcal{I}_{k+P}}\mathbf{M}$. Note that $\mathbf{P}_{\mathcal{I}_{K-2}}$ projects onto the space orthogonal to $\mathsf{span}(\mathbf{G}_{\mathcal{I}_{K-1}})$, while $\mathbf{M}^T\mathbf{W}_{k+1}$ has $K-(k+1)-(P-1)$ number of sub-channels that are orthogonal to $\mathsf{span}(\mathbf{G}_{\mathcal{I}_{K-1}})$ and the remaining $(P-1)$ sub-channels would have components in the $\mathsf{span}(\mathbf{G}_{\mathcal{I}_{K-1}})$. When $K \gg P$, we will have a large number of subchannels in $\mathbf{M}^T\mathbf{W}_{k+1}$ that are orthogonal to $\mathsf{span}(\mathbf{G}_{\mathcal{I}_{K-1}})$ and hence $\mathbf{P}_{\mathcal{I}_{K-2}}\mathbf{M}^T\mathbf{W}_{k+1} \approx \mathbf{M}^T\mathbf{W}_{k+1}$ for $0 \le k < K-P-1$. Thus, even for a finite value of K we can expect a large number of sub-channels to be essentially identical, which is validated by our simulation results presented in Fig. 4 in the later part of the paper.

We can infer from Proposition 3 that the parallel sub-channels are essentially the same, when $K \gg P$ and hence we can expect only a few distinct TA subsets in $\mathcal{A}_{SIC}$ upon employing Algorithm 1. We now analyse Algorithm 1 by considering several statistical metrics and validate the theoretical insights with the aid of numerical investigations.

Let D represent the number of distinct elements in $\mathcal{A}_{SIC}$, where $1 \le D \le \binom{N_t}{N_{SM}}$ and $P_D(l)$ represent the percentage of occurrence of the l^{th} majority elements[2] in $\mathcal{A}_{SIC}$. Then, $P_D(1)$ represents the percentage of occurrence of the majority elements in $\mathcal{A}_{SIC}$ and $P_D(2)$ represents the percentage of occurrence of the second largest majority elements, so on and so forth. We study

- the cumulative distribution function (CDF) of D, i.e. $F_D(d) = Pr(D \le d)$, which allows us to quantify the number of distinct elements in the set $\mathcal{A}_{SIC}$, and
- the average $P_D(l)$ for $l = 1, 2, \ldots$ which enables us to quantify the distribution of the size of the majority sets in $\mathcal{A}_{SIC}$,

both evaluated using Monte Carlo simulations.

Consider a ZP-SC SM system having $N_t = N_r = 6$, $N_{SM} = 4$, $K = 8$ and employing SIC-TAS for a 32-QAM signal set. Fig. 2(a) depicts the variation in $F_D(d)$ for the values of $\beta \in \{0.2, 0.4, 0.8\}$, whereas Fig. 2(b) corresponds to the variation in $P_D(l)$. The three values of β considered above correspond to the fast, moderate and slow channel impulse response (CIR) decay scenarios, respectively. It is evident from Fig. 2(a) that for any value of β, we have $F_D(d) = Pr(D \le d) \approx 1$ for d as small as four, which means that no more than four distinct TA subsets occur on average in the set $\mathcal{A}_{SIC}$. Furthermore, we observe from Fig. 2(b) that a single antenna subset constitutes at least 75% of the antenna subsets in $\mathcal{A}_{SIC}$, regardless of the specific channel decay factor β, thanks to the nearly identical parallel sub-channels due to Partial-SIC. It can be observed from Fig. 2(b) that for the moderate value of $\beta = 0.4$, the majority set constitutes 84%, whereas the second majority set constitutes less than 15%.

[2]Please refer to *Notations* for the definition of the majority element.

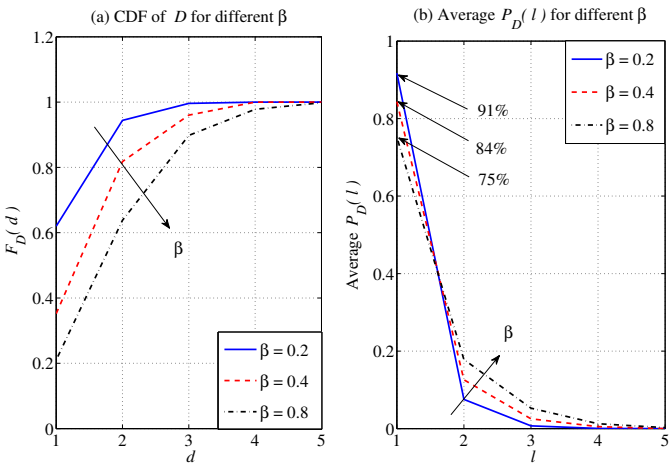

Fig. 2. Plot (a) depicts the CDF of D for various values of channel decay factor β in a ZP-SC SM system. The system is assumed to have $N_t = N_r = 6$, $N_{SM} = 4$, $K = 8$, $P = 4$ and employing SIC-TAS with 32-QAM. Plot (b) corresponds to the variation of $P_D(l)$ in the aforementioned system.

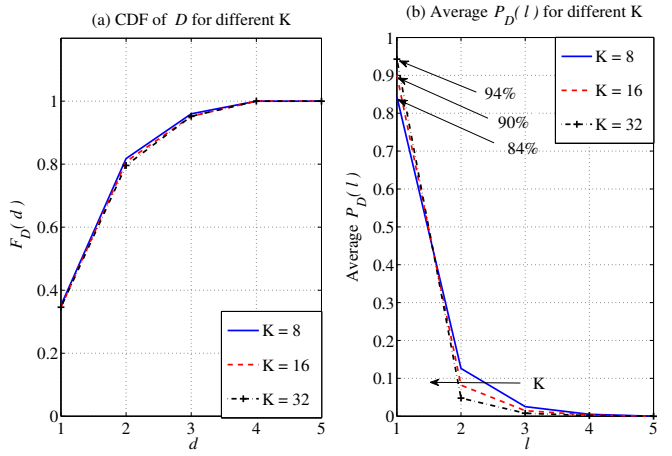

Fig. 3. Plot (a) depicts the CDF of D for various values of data frame length K in a ZP-SC SM system. The system is assumed to have $N_t = N_r = 6$, $N_{SM} = 4$, $\beta = 0.4$, $P = 4$ and employing SIC-TAS with 32-QAM. Plot (b) corresponds to the variation of $P_D(l)$ in the aforementioned system.

Figure 3 depicts the variation in $F_D(d)$ and $P_D(l)$ with respect to K, where the CIR decay factor is fixed to be $\beta = 0.4$. It is evident from Fig. 3(a) that the number of distinct sets remains almost the same for any value of K. Fig. 3(b) shows that the size of the majority set grows with K, as predicted by Proposition 3. Specifically, when $K = 32$, the majority set constitutes 94% of the set $\mathcal{A}_{SIC}$, while the second majority set constitutes less than 5%. Thus, by having a sufficiently large K, we can ensure that a single TA subset constitutes nearly the entire $\mathcal{A}_{SIC}$.

The above findings motivate us to consider a majority based TA subset selection, which enables us to have a single antenna subset for all the K channel uses and in turn utilise only $\log_2(\lceil \binom{N_t}{N_{SM}} \rceil_{2^p})$ bits in the feedback channel, which reduces the feedback overhead in the frequency selective scenario to that of the flat-fading scenario. In case of majority decision

based TA subset selection, the antenna subset to be used in all the K channel uses of the data frame is given by

$$\mathcal{A}_{MAJ-TAS} = \mathsf{maj}(\mathcal{A}_{SIC}). \tag{46}$$

This selection scheme is referred to as MAJ-TAS. Although the MAJ-TAS scheme reduces the feedback overhead, it still requires $\mathcal{A}_{SIC}$ to be computed, which is computationally expensive. In order to alleviate this issue, we have to understand the variation in $Pr(\mathcal{A}_k \neq \mathcal{A}_{MAJ-TAS})$ over $0 \leq k \leq K-1$, so that we can avoid computing the entire set $\mathcal{A}_{SIC}$. Specifically, we look for a subset $\mathcal{K} \subset \{i\}_{i=0}^{K-1}$ such that $Pr(\mathcal{A}_k \neq \mathcal{A}_{MAJ-TAS}) \leq \epsilon$ for $k \in \mathcal{K}$ for a small positive ϵ.

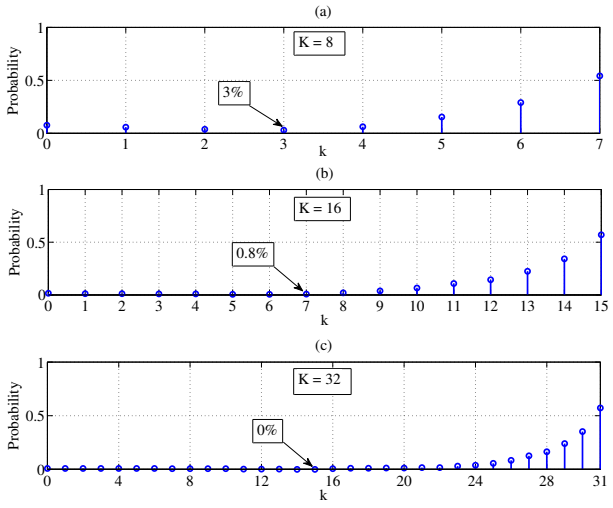

Fig. 4. Plot (a)-(c) depict the $Pr(\mathcal{A}_k \neq \mathcal{A}_{MAJ-TAS})$ for various values of K in a ZP-SC SM system. The system is assumed to have $N_t = N_r = 6$, $N_{SM} = 4$, $\beta = 0.4$, $P = 4$ and employing SIC-TAS with 32-QAM.

Figure 4 depicts the $Pr(\mathcal{A}_k \neq \mathcal{A}_{MAJ-TAS})$ for various values of K. It is evident from Fig. 4(a)-(c) that the $Pr(\mathcal{A}_k \neq \mathcal{A}_{MAJ-TAS})$ is very small for $k < K/2$ and slowly increases, as k approaches $K-1$. Thus, by taking $\mathcal{K} = \{K/2 - i\}_{i=1}^{L}$ we propose a low-complexity MAJ-TAS scheme termed as L-MAJ-TAS:

$$\mathcal{A}_{L-MAJ-TAS} = \mathsf{maj}\{\mathcal{A}_{K/2-L}, \ldots, \mathcal{A}_{K/2-2}, \mathcal{A}_{K/2-1}\}. \tag{47}$$

Note that (47) requires (11) to be computed only L times, whereas (46) requires (11) to be computed K times. Furthermore, it is evident from Fig. 4 that as K becomes large, the $Pr(\mathcal{A}_k \neq \mathcal{A}_{MAJ-TAS})$ tends to zero, which further validates Proposition 3. We will show in Section IV that $L = 1$ would be sufficient to attain the same performance as that of the SIC-TAS scheme with $L = K$. Although it is desirable to have a large K, it cannot be made arbitrarily large, since the clock drift at both the transmitter as well as at the receiver would require the periodic availability of reference signals, which in turn determines the value of K. Given P, a reasonable value of K may vary from $4P$ to $8P$.

B. The Proposed MU-TAS Algorithm

We first generalise the Partial-SIC [6] to the multiuser scenario to obtain MU-SIC, which enables us to mitigate both the inter-user and inter-channel interferences. The proposed MU-SIC is presented in Algorithm 2.

Algorithm 2 MU-SIC for the multiuser ZP-SC SM system

Require: $u = 1$.
  while $u \leq U$ **do**
    $\mathbf{T}^{(u)} = \left[\hat{\mathbf{H}}^{(u+1)}, \hat{\mathbf{H}}^{(u+2)}, \ldots, \hat{\mathbf{H}}^{(U)}\right]$, $k = 0$.
    while $k < K$ **do**
      1. $\bar{\mathbf{G}}_{\mathcal{I}_k}^{(u)} = \left[\mathbf{G}_{\mathcal{I}_{k+1}}^{(u)}, \ldots, \mathbf{G}_{\mathcal{I}_{K-1}}^{(u)}, \mathbf{T}^{(u)}\right]$,
        $\mathbf{Q}_{\mathcal{I}_k}^{(u)} = \bar{\mathbf{G}}_{\mathcal{I}_k}^{(u)} \left((\bar{\mathbf{G}}_{\mathcal{I}_k}^{(u)})^H \bar{\mathbf{G}}_{\mathcal{I}_k}^{(u)}\right)^{-1} (\bar{\mathbf{G}}_{\mathcal{I}_k}^{(u)})^H$,
        $\mathbf{P}_{\mathcal{I}_k}^{(u)} = \mathbf{I}_{N_r(K+P-1)} - \mathbf{Q}_{\mathcal{I}_k}^{(u)}$.
      2. Obtain
        $\mathbf{z}_{\mathcal{I}_k}^{(u)} = \mathbf{P}_{\mathcal{I}_k}^{(u)} \hat{\mathbf{y}}$,
        $\tilde{\mathbf{x}}_k^{(u)} = \arg\min_{\mathbf{x} \in \mathcal{X}_k^{(u)}} \|\mathbf{z}_{\mathcal{I}_k}^{(u)} - \mathbf{P}_{\mathcal{I}_k}^{(u)} \mathbf{G}_{\mathcal{I}_k}^{(u)} \mathbf{x}\|^2$,
        $\hat{\mathbf{y}} \leftarrow \hat{\mathbf{y}} - \mathbf{G}_{\mathcal{I}_k}^{(u)} \tilde{\mathbf{x}}_k^{(u)}$,
        $k \leftarrow k + 1$.
    end while
    $u \leftarrow u + 1$.
  end while

Note that Algorithm 2 is similar to Partial-SIC [6], except that in addition to the inter-channel interference, the inter-user interference is also taken into account, which is captured by $\mathbf{T}^{(u)}$ in Algorithm 2. Furthermore, the MU-SIC only becomes feasible when the number of receive antennas at the BS is sufficiently large. Hence, we have to have $UKN_t \leq N_r(K+P-1)$ in order to employ the MU-SIC. In other words, when K is large, we have to ensure that $N_r \geq UN_t$ in order to support U users. Note that this may not be an issue, since the BS can be equipped with a large number of antennas in contrast to the users' equipment, which have limited form factor.

The proposed MU-TAS is presented in Algorithm 3, which exploits the MU-SIC in order to arrive at the optimal antenna subsets $\{\mathcal{A}_{SIC}^{(u)}\}_{u=1}^{U}$ for each of the users. Note that when $U = 1$, the MU-TAS presented in Algorithm 3 reduces to the SIC-TAS presented in Algorithm 1. Furthermore, note that the order of computational complexity of Algorithm 1 is given by $\mathcal{O}(N_t^3 K \log^2 K)$ (Section IV-B [6]). The order of computational complexity of Algorithm 3 scales at least as fast as $\mathcal{O}(N_t^3 U^3 K \log^2 K)$. Thus, the computational complexity of the proposed MU-TAS algorithm scales at least cubically with the number of users U in comparison to the single user scenario.

Let us now study the signal and interference spaces in the case of multiple users. Let $k \gg P$, $\mathbf{U}_k^{(j)} = \left[\mathbf{G}_{\mathcal{I}_{k-P+1}}^{(j)}, \ldots, \mathbf{G}_{\mathcal{I}_{k-1}}^{(j)}, \mathbf{G}_{\mathcal{I}_k}^{(j)}, \mathbf{G}_{\mathcal{I}_{k+1}}^{(j)}, \ldots, \mathbf{G}_{\mathcal{I}_{k+P-1}}^{(j)}\right]$ represent the inter-user interference due to the j^{th} user in the k^{th} channel use. In order to gain insight into the nature of parallel sub-channels in the MU-TAS of Algorithm 3, let us partition $\bar{\mathbf{G}}_{\mathcal{I}_k}^{(u)}$ into $[\mathbf{J}_k^{(u)}, \mathbf{W}_k^{(u)}]$, where $\mathbf{J}_k = \left[\mathbf{G}_{\mathcal{I}_{k+1}}^{(u)}, \ldots, \mathbf{G}_{\mathcal{I}_{k+P-1}}^{(u)}, \cup_{j=u+1}^{U} \mathbf{U}_k^{(j)}\right]$ corresponds

Algorithm 3 MU-TAS for the multiuser ZP-SC SM system

Require: $u = 1$.
  while $u \leq U$ **do**
    $\mathbf{T}^{(u)} = \left[\hat{\mathbf{H}}^{(u+1)}, \hat{\mathbf{H}}^{(u+2)}, \ldots, \hat{\mathbf{H}}^{(U)}\right]$, $\mathcal{A}_{SIC}^{(u)} = \{\cdot\}$, $k = 0$.
    while $k < K$ **do**
      1. $\bar{\mathbf{G}}_{\mathcal{I}_k}^{(u)} = \left[\mathbf{G}_{\mathcal{I}_{k+1}}^{(u)}, \ldots, \mathbf{G}_{\mathcal{I}_{K-1}}^{(u)}, \mathbf{T}^{(u)}\right]$,
        $\mathbf{Q}_{\mathcal{I}_k}^{(u)} = \bar{\mathbf{G}}_{\mathcal{I}_k}^{(u)} \left((\bar{\mathbf{G}}_{\mathcal{I}_k}^{(u)})^H \bar{\mathbf{G}}_{\mathcal{I}_k}^{(u)}\right)^{-1} (\bar{\mathbf{G}}_{\mathcal{I}_k}^{(u)})^H$,
        $\mathbf{P}_{\mathcal{I}_k}^{(u)} = \mathbf{I}_{N_r(K+P-1)} - \mathbf{Q}_{\mathcal{I}_k}^{(u)}$,
        $\mathbf{R}_k^{(u)} = \mathbf{P}_{\mathcal{I}_k}^{(u)} \mathbf{G}_{\mathcal{I}_k}^{(u)}$.
      2. Obtain

$$\mathcal{A}_k^{(u)} = \arg \max_{\substack{\mathcal{A}' \subset \mathcal{A}, \\ |\mathcal{A}'| = N_{SM}}} \min_{\mathbf{x}_1 \neq \mathbf{x}_2} \|\mathbf{R}_k^{(u)}(:, \mathcal{A}')(\mathbf{x}_1 - \mathbf{x}_2)\|^2,$$

        $\mathcal{A}_{SIC}^{(u)} \leftarrow \mathcal{A}_{SIC}^{(u)} \cup \mathcal{A}_k^{(u)}$,
        $k \leftarrow k + 1$.
    end while
    $\mathcal{A}_{MU-TAS} \leftarrow \mathcal{A}_{MU-TAS} \cup \mathcal{A}_{SIC}^{(u)}$,
    $u \leftarrow u + 1$.
  end while

to the sub-channels that interfere with $\mathbf{G}_{\mathcal{I}_k}^{(u)}$ due to inter-channel and inter-user interference, while $\mathbf{W}_k = \left[\mathbf{G}_{\mathcal{I}_{k+P}}^{(u)}, \ldots, \mathbf{G}_{\mathcal{I}_{K-1}}^{(u)}, \cup_{j=1}^{U} \{\mathbf{G}_{\mathcal{I}_k}^{(j)}\}_{k=0}^{K-1} \backslash \mathbf{U}_k^{(j)}\right]$ corresponds to the sub-channels that are orthogonal to $\mathbf{G}_{\mathcal{I}_k}^{(u)}$. Proceeding along the lines of Proposition 2, it can be shown that

$$\mathbf{P}_{\mathcal{I}_k}^{(u)} \mathbf{G}_{\mathcal{I}_k}^{(u)} \equiv \left[\mathbf{I} - \mathsf{Proj}[(\mathbf{I} - \mathsf{Proj}(\mathbf{W}_k^{(u)}))\mathbf{J}_k^{(u)}]\right] \mathbf{G}_{\mathcal{I}_k}^{(u)}. \quad (48)$$

For any given u, we have $\mathbf{J}_k^{(u)} \equiv \mathbf{J}_{k+1}^{(u)}$, $\mathbf{W}_k^{(u)} \equiv \mathbf{W}_{k+1}^{(u)}$, and $\mathbf{G}_{\mathcal{I}_k}^{(u)} \equiv \mathbf{G}_{\mathcal{I}_{k+1}}^{(u)}$ except for the shift, when $K \to \infty$. As a result, we have $\mathbf{P}_{\mathcal{I}_k}^{(u)} \mathbf{G}_{\mathcal{I}_k}^{(u)} \to \mathbf{M}^T \mathbf{P}_{\mathcal{I}_k}^{(u)} \mathbf{G}_{\mathcal{I}_k}^{(u)}$ when $K \to \infty$ and $k \gg P$. Thus, the parallel sub-channels are nearly the same even in case of the multi-user scenario, provided that K is sufficiently large. Let us now validate the above observations by considering a MU-TAS aided ZP-SC SM system serving two users ($U = 2$), where both users' signals are assumed to have the same received power at the BS. Let the number of receive antennas at the BS be $N_r = 6$ and the number of TAs at each of the two users be $N_t = 3$ and $N_{SM} = 2$. Both users be assumed to be employing 32-QAM and operating in a frequency selective channel having $\beta = 0.4$ and $P = 4$ with the aid of the ZP-SC SM system using $K = 8$ and employing MU-TAS. Note that only the first user suffers from the inter-user interference, while the second user does not, as a benefit of the SIC. Thus, we explicitly study the first user's $F_D(d) = Pr(D \leq d)$ and $P_D(l)$. Figure 5 depicts the variation in $F_D(d)$ and $P_D(l)$ with respect to K in the first user's case. It is evident from Fig. 5(a) that the number of distinct sets remains almost the same for any value of K. Fig. 5(b) shows that the size of the majority set grows with K, which is in accordance with the above analysis. Specifically, when $K = 32$ the majority set constitutes 95% of the set $\mathcal{A}_{SIC}^{(1)}$, while the second majority set constitutes less than 5%.

Thus, by having a sufficiently large K, we can ensure that a single TA subset constitutes nearly the entire $\mathcal{A}_{SIC}^{(1)}$. Hence, analogous to the single user scenario, we may have

$$\mathcal{A}_{MAJ-TAS}^{(u)} = \mathsf{maj}(\mathcal{A}_{SIC}^{(u)}), \quad (49)$$

which is termed as MAJ-MU-TAS.

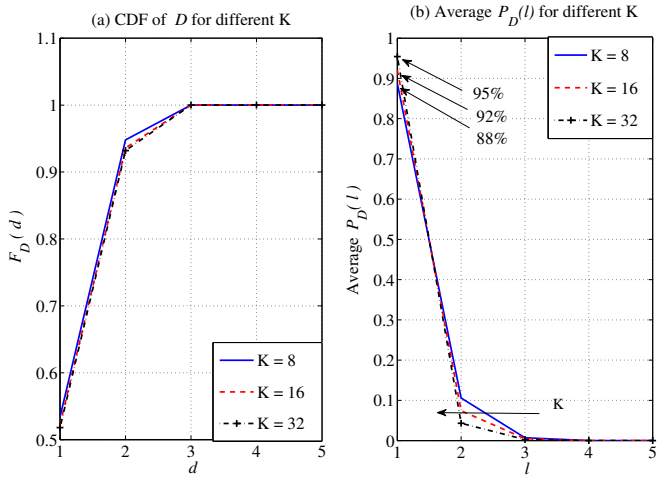

Fig. 5. Plot (a) depicts the CDF of D for various values of data frame length K of the first user in a two-user ($U = 2$) ZP-SC SM system. The system is assumed to have $N_r = 6$, $N_t = 3$, $N_{SM} = 2$, operating in a frequency selective channel having $\beta = 0.4$, $P = 4$ and employing MU-TAS with 32-QAM. Plot (b) corresponds to the variation of $P_D(l)$ in the aforementioned system.

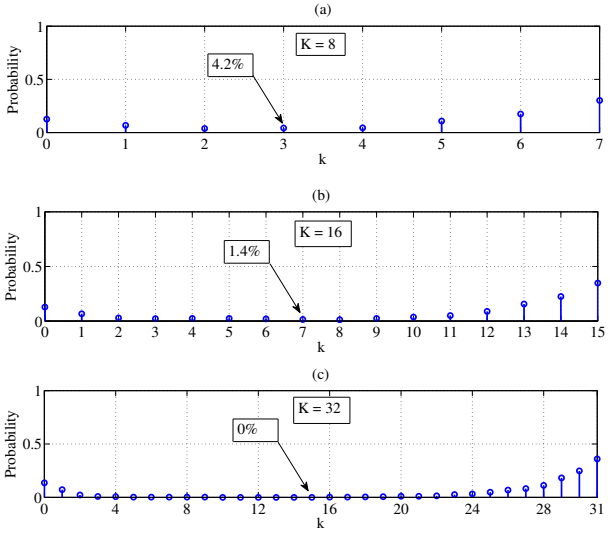

Fig. 6. Plot (a)-(c) depict the $Pr(\mathcal{A}_k^{(u)} \neq \mathcal{A}_{MAJ-TAS}^{(u)})$ for various values of K of the first user in a two-user ($U = 2$) ZP-SC SM system. The system is assumed to have $N_r = 6$, $N_t = 3$, $N_{SM} = 2$, operating in a frequency selective channel having $\beta = 0.4$, $P = 4$ and employing MU-TAS with 32-QAM signal set.

Figure 6 depicts the $Pr(\mathcal{A}_k^{(u)} \neq \mathcal{A}_{MAJ-TAS}^{(u)})$ for various values of K. It is evident from Fig. 6(a)-(c) that the $Pr(\mathcal{A}_k^{(u)} \neq \mathcal{A}_{MAJ-TAS}^{(u)})$ is very small for $k \approx K/2$ and

increases slowly as k deviates from $K/2$. Thus, by taking $\mathcal{K} = \{K/2 - i\}_{i=1}^{L}$ we propose a low-complexity MAJ-TAS scheme for the multi-user scenario:

$$\mathcal{A}_{L-MAJ-TAS}^{(u)} = \mathsf{maj}\{\mathcal{A}_{K/2-L}^{(u)}, \ldots, \mathcal{A}_{K/2-2}^{(u)}, \mathcal{A}_{K/2-1}^{(u)}\}, \tag{50}$$

which is termed as L-MAJ-MU-TAS. Analogous to the single user scenario, we will demonstrate in Section IV that $L = 1$ would be sufficient to attain the same performance as that of the MU-TAS with $L = K$. In the next section, we study the BER performance of the proposed TAS schemes.

IV. Simulation Results and Discussions

Simulation scenario: In all our simulations, we have employed at least 10^{t+1} bits for evaluating a BER of 10^{t}. All the simulation results are obtained by considering a frequency selective channel having $\beta = 0.4$ and $P = 2$, and the ZP-SC SM system is assumed to be operating with a frame length of $K = 8$. The receiver is assumed to have perfect CSI in all the detection algorithms considered.

A. Performance of TAS Schemes in Single User Scenario

Consider a ZP-SC SM system employing the SIC-TAS algorithm in conjunction with 32- and 64-QAM signal sets. Let us consider two system configurations: a) $N_r = N_t = 4$ and $N_{SM} = 2$; and b) $N_r = N_t = 6$ and $N_{SM} = 4$. Figure 7 compares the BER performance of the aforementioned system in both the configurations against their counterparts, where no TAS is employed. Specifically, Fig. 7(a) and Fig. 7(b) compare the BER performance in the configurations a) and b), respectively. The observations from Fig. 7 are listed as follows:

- In both the configurations, the system employing SIC-TAS attains a better BER performance than that which does not. Specifically, at a BER of 10^{-5} there is an SNR gain of about 3dB in case of 32-QAM and of about 2dB in case of 64-QAM in configuration a). Furthermore, there is an SNR gain of about 1dB in case of both the 32- and 64-QAM signal sets in configuration b).
- Note that when N_r is increased, the overall diversity gain of the system is also increased. Since the diversity gain is a high SNR phenomenon, we need higher SNR to see the benefits of increased diversity gain. Thus, in Fig. 7(b) where $N_r = 6$, we do not see any significant improvement in the performance gain. This is analogous to the marginal improvement in the performance benefit of TAS in the low SNR range (4dB to 12dB) of Fig. 7(a).
- The gain in the SNR due to TAS diminishes as the size of the signal set is increased. This is expected, since the minimum ED in the received signal space diminishes, as the constellation size is increased.

Figure 8 compares the BER performance of the ZP-SC SM system employing the SIC-TAS algorithm in conjunction with 32-QAM signal set, where the channel parameters are assumed to be $P = 3$, $K = 12$, and $\beta = 0.4$. It is evident from Fig. 8 that the TAS aided SM provides better performance, when compared to its counterpart operating without TAS.

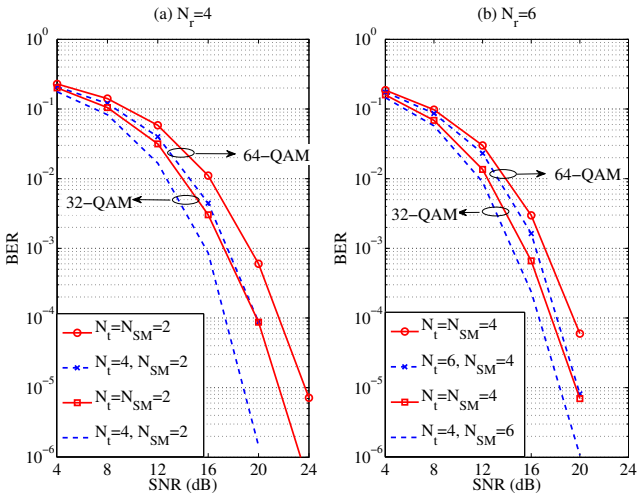

Fig. 7. Comparison of the BER performance in the ZP-SC SM system having $K = 8$ and employing SIC-TAS. When employing SIC-TAS, $N_r = N_t = 4$, $N_{SM} = 2$ are used in conjunction with 32- and 64-QAM signal sets, which correspond to Plot (a). Plot (b) corresponds to the case, where $N_r = N_t = 6$ and $N_{SM} = 4$.

Specifically, at a BER of 10^{-5} there is an SNR gain of about 2dB in case of configuration a). Furthermore, there is an SNR gain of about 1dB in case of configuration b).

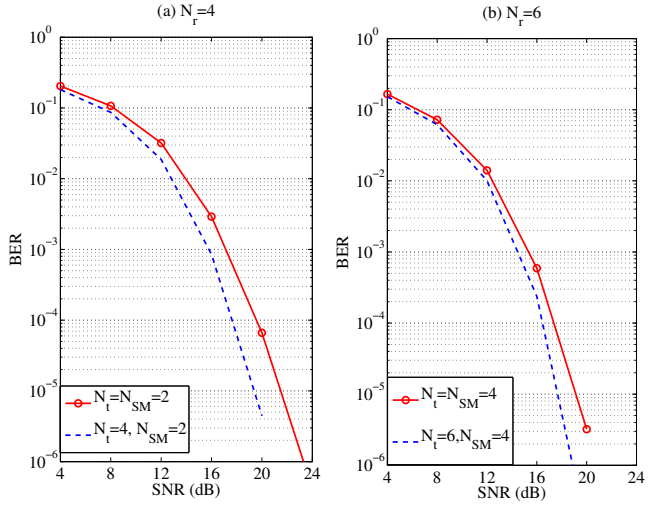

Fig. 8. Comparison of the BER performance in the ZP-SC SM system having $K = 12$ and employing SIC-TAS. When employing SIC-TAS, $N_r = N_t = 4$, $N_{SM} = 2$ are used in conjunction with 32-QAM signal set, which correspond to Plot (a). Plot (b) corresponds to the case, where $N_r = N_t = 6$ and $N_{SM} = 4$. The frequency selective channel is assumed to have $\beta = 0.4$ and $P = 3$.

Figure 9 compares the various TAS schemes proposed in the paper. Explicitly, the SIC-TAS, MAJ-TAS, and L-MAJ-TAS with $L = 1$ are compared in both the configurations considered above. It is evident from Fig. 9(a) and Fig. 9(b) that the MAJ-TAS and 1-MAJ-TAS attain the same performance as that attained by the SIC-TAS. Thus, the low-complexity version of the SIC-TAS, i.e. the 1-MAJ-TAS, is sufficient for attaining the performance gains guaranteed by TA subset selection.

Fig. 10 compares the BER performance of the aforementioned schemes in a channel having $\beta = 0.8$ in contrast to that of Fig. 9, where $\beta = 0.4$. It is evident from Fig. 10 that there is negligible performance loss in the proposed low-complexity 1-MAJ-TAS scheme compared to the SIC-TAS and MAJ-TAS schemes in both the cases considered in Fig. 10(a) and Fig. 10(b). Thus, we conclude that the proposed scheme is robust to the variation in the channel's decay parameter β.

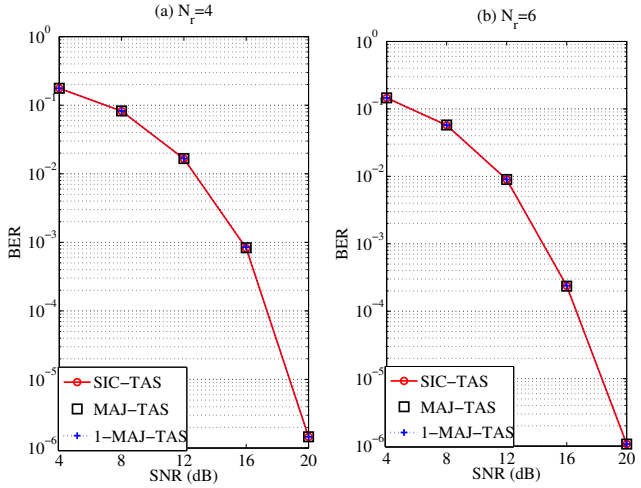

Fig. 9. Comparison of the BER performance in the ZP-SC SM system having $K = 8$ and employing SIC-TAS, MAJ-TAS and L-MAJ-TAS with $L = 1$ (1-MAJ-TAS). The Plot (a) corresponds to the case where $N_t = N_r = 4$ and $N_{SM} = 2$, while the Plot (b) corresponds to the case where $N_t = N_r = 6$ and $N_{SM} = 4$.

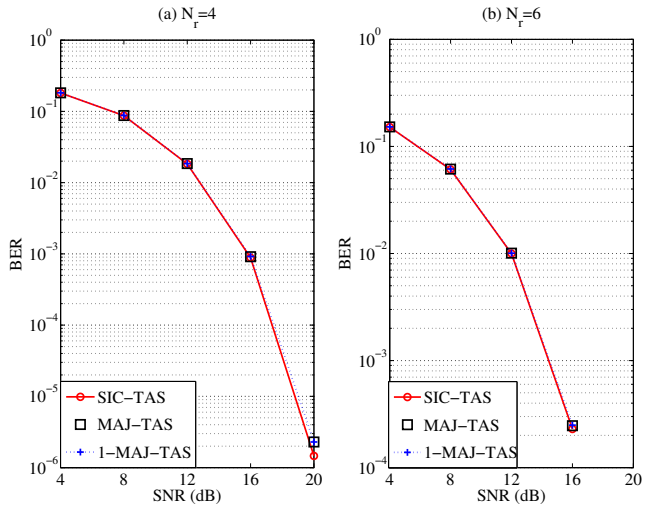

Fig. 10. Comparison of the BER performance in the ZP-SC SM system having $K = 8$ and employing SIC-TAS, MAJ-TAS and L-MAJ-TAS with $L = 1$ (1-MAJ-TAS). Plot (a) corresponds to the case where $N_t = N_r = 4$ and $N_{SM} = 2$, while the Plot (b) corresponds to the case where $N_t = N_r = 6$ and $N_{SM} = 4$. The channel decay parameter β is assumed to be 0.8 in both the cases.

Remark 2: It is worth noting that although MAJ-TAS and 1-MAJ-TAS employ antenna subsets that are not optimal, especially for sub-channels that are close to the K^{th} sub-channel (refer Fig. 4), they attain essentially the same performance as that of the SIC-TAS. This is due to the fact that the sub-channels that are close to the K^{th} sub-channel experience less interference and as such do not significantly benefit from the antenna selection, whereas the sub-channels that are farther from the K^{th} sub-channel experience severe interference and hence they predetermine the performance of the system.

Let us now compare the BER performance of the 1-MAJ-TAS scheme using various equalization algorithms. Figure 11 compares the BER performance of 1-MAJ-TAS in both the configurations mentioned earlier, where Partial-SIC, PIC-R [6], zero forcing (ZF) and minimum mean square error (MMSE) equalizers are employed. It is evident from Fig. 11 that the PIC-R, ZF, and MMSE equalization result in a performance degradation compared to the Partial-SIC case. This indicates that the beneficial distance properties attained with the aid of Partial-SIC are not retained, when equalization algorithms other than the Partial-SIC are employed. This is so, since the symmetry in the interference present in the case of Partial-SIC will not be present in the case of other equalization schemes, such as ZF and MMSE. Furthermore, in addition to the benefit of nearly identical parallel sub-channels, the Partial-SIC gives the best performance compared to the other equalization schemes. This is mainly due to the reduced level of interference experienced by the various sub-channels owing to the SIC.

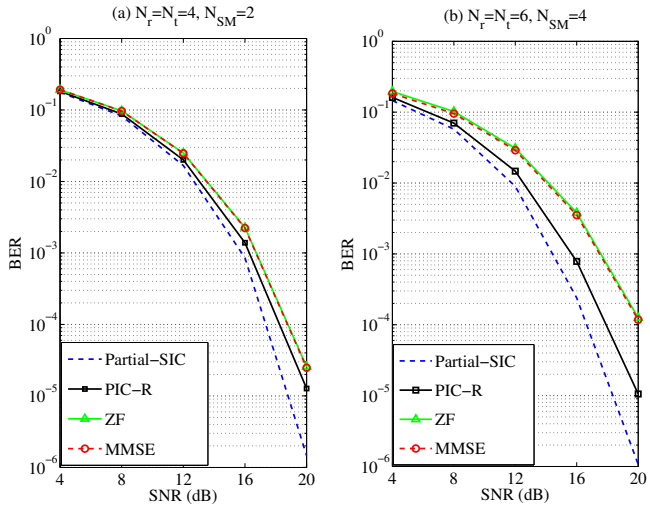

Fig. 11. Comparison of the BER performance in the ZP-SC SM system having $K = 8$ and employing Partial-SIC, PIC-R, ZF and MMSE detectors. The Plot (a) corresponds to the case where $N_t = N_r = 4$ and $N_{SM} = 2$, while the Plot (b) corresponds to the case where $N_t = N_r = 6$ and $N_{SM} = 4$. Both the systems are assumed to be employing L-MAJ-TAS with $L = 1$ (1-MAJ-TAS).

B. Performance of TAS Schemes in Multi-User Scenario

Consider a two user ($U = 2$) ZP-SC SM system employing the MU-TAS algorithm in conjunction with the 64-QAM signal set. Let $N_r = 6, N_t = 3$ or 2 and $N_{SM} = 2$. The case of $N_t = 2$ corresponds to the *No TAS* scenario and the case of $N_t = 3$ corresponds to the *MU-TAS* scenario. Figure 12

compares the attainable BER performance of both the users in the *No TAS* and *MU-TAS* scenarios, when employing the 64-QAM signal set. It is evident from Fig. 12 that the *MU-TAS* outperforms the *NO TAS* scenario in case of both the users. Specifically, an SNR gain of about 1dB is observed in case of user 2 at a BER of 2×10^{-5}. Furthermore, the BER performance of user 2 is observed to be better than that of user 1 by about 4dB at a BER of 10^{-4} in case of *MU-TAS*. Furthermore, in case of user 2 an SNR gain of about 1dB is observed, when employing *MU-TAS* compared to the *No TAS* scenario.

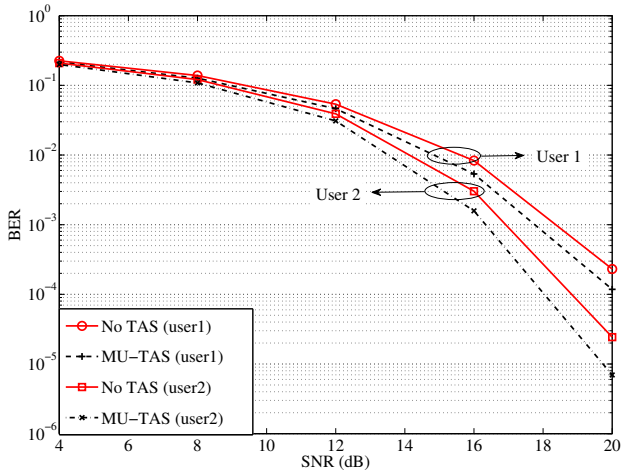

Fig. 12. Comparison of the BER performance in a two user ($U = 2$) ZP-SC SM system. The system is assumed to have $K = 8$ and employing MU-TAS. When employing MU-TAS, $N_r = 6, N_t = 3$, $N_{SM} = 2$ are used in conjunction with 64-QAM signal set.

Fig. 13 compares the BER performance of various multiuser TAS schemes proposed in the paper, such as MU-TAS, MAJ-MU-TAS, and L-MAJ-MU-TAS. It is evident from Fig.13 that both the MAJ-MU-TAS and 1-MAJ-MU-TAS scheme attain nearly the same performance as that of MU-TAS. Thus, using the 1-MAJ-MU-TAS, which imposes both minimal feedback overhead and computational burden, is sufficient to attain the same performance as that of the MU-TAS. Specifically, the 1-MAJ-MU-TAS scheme requires ED-TAS to be invoked over only one of the sub-channels for each user and hence substantially reduces the computational complexity. Furthermore, since only one optimal TA subset is used across all the sub-channels, the feedback overhead per user is the same as that of the flat-fading scenario.

V. Conclusions

We have proposed TAS schemes for single- and multi-user ZP-SC SM systems operating in a frequency selective channel, which has hitherto not been studied in the literature. Specifically, the frequency selective channel of a single user is first converted into a set of non-interfering parallel sub-channels by employing Partial-SIC. Then the ED-TAS technique is invoked for each of the parallel sub-channels in order to improve the attainable system performance. The parallel

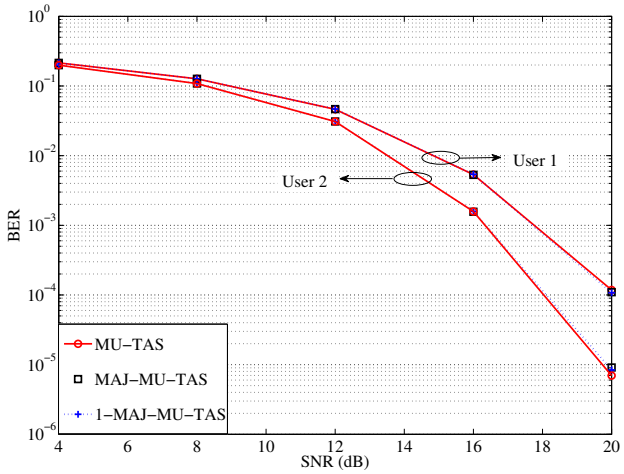

Fig. 13. Comparison of the BER performance in a two user ($U = 2$) ZP-SC SM system. The system is assumed to have $K = 8$ and employing MU-TAS, MAJ-MU-TAS and L-MAJ-MU-TAS with $L = 1$ (1-MAJ-MU-TAS). Both the users are assumed to have $N_t = 3$ and $N_{SM} = 2$.

sub-channels of the Partial-SIC are theoretically shown to be nearly identical, which enabled us to reduce both the feedback overhead and the computational complexity of ED-TAS over each of the sub-channels. Furthermore, the theoretical insights were validated by numerical simulations, which confirmed that a large percentage of sub-channels indeed have the same ED-TAS optimal TA subset, resulting in reduced feedback overhead and computational complexity. The proposed single-user TAS schemes were extended to a multiuser scenario, where beneficial performance gains were observed in comparison to the *No TAS* counterparts. Specifically, a performance gain as high as 3dB was observed in the single-user scenario and of about 1dB in case of the two-user scenario, when employing TAS. While our study has mainly focused on SM systems having moderate number of transmit and receive antennas, the antenna selection problem in SM systems employing massive number of antennas is largely unexplored and it would be a promising topic for future research.

VI. Appendix A
Closed form expression of $\mathbf{P}_{\mathcal{I}_{k+P-1}}$

Since $\mathbf{W}_k = [\mathbf{M}^T\mathbf{W}_{k+1}\ \mathbf{G}_{\mathcal{I}_{K-1}}]$, we have

$$\mathbf{Q}_{\mathcal{I}_{k+P-1}} = \mathbf{W}_k(\mathbf{W}_k^H\mathbf{W}_k)^{-1}\mathbf{W}_k^H, \tag{51}$$

$$= \left[\mathbf{M}^T\mathbf{W}_{k+1}\ \mathbf{G}_{\mathcal{I}_{K-1}}\right] \times \begin{bmatrix} \mathbf{W}_{k+1}^H\mathbf{M}\mathbf{M}^T\mathbf{W}_{k+1} & \mathbf{W}_{k+1}^H\mathbf{M}\mathbf{G}_{\mathcal{I}_{K-1}} \\ \mathbf{G}_{\mathcal{I}_{K-1}}^H\mathbf{M}^T\mathbf{W}_{k+1} & \mathbf{G}_{\mathcal{I}_{K-1}}^H\mathbf{G}_{\mathcal{I}_{K-1}} \end{bmatrix}^{-1} \times \begin{bmatrix} \mathbf{W}_{k+1}^H\mathbf{M} \\ \mathbf{G}_{\mathcal{I}_{K-1}}^H \end{bmatrix}, \tag{52}$$

$$= \left[\mathbf{M}^T\mathbf{W}_{k+1}\ \mathbf{G}_{\mathcal{I}_{K-1}}\right] \begin{bmatrix} \mathbf{A} & \mathbf{B} \\ \mathbf{C} & \mathbf{D} \end{bmatrix} \begin{bmatrix} \mathbf{W}_{k+1}^H\mathbf{M} \\ \mathbf{G}_{\mathcal{I}_{K-1}}^H \end{bmatrix}, \tag{53}$$

$$= \mathbf{M}^T\mathbf{W}_{k+1}\mathbf{A}\mathbf{W}_{k+1}^H\mathbf{M} + \mathbf{G}_{\mathcal{I}_{K-1}}\mathbf{C}\mathbf{W}_{k+1}^H\mathbf{M} + \mathbf{M}^T\mathbf{W}_{k+1}\mathbf{B}\mathbf{G}_{\mathcal{I}_{K-1}}^H + \mathbf{G}_{\mathcal{I}_{K-1}}\mathbf{D}\mathbf{G}_{\mathcal{I}_{K-1}}^H. \tag{54}$$

Since $\mathbf{G}_{\mathcal{I}_{K-1}} \perp \mathbf{J}_k$, we can ignore the last two terms in (54). By invoking the block matrix inversion lemma of [44], we have

$$\mathbf{A} = (\mathbf{W}_{k+1}^H \mathbf{M} \mathbf{P}_{\mathcal{I}_{K-2}} \mathbf{M}^T \mathbf{W}_{k+1})^{-1}, \tag{55}$$

$$\mathbf{C} = -(\mathbf{G}_{\mathcal{I}_{K-1}}^H \mathbf{G}_{\mathcal{I}_{K-1}})^{-1} \mathbf{G}_{\mathcal{I}_{K-1}}^H \mathbf{M}^T \mathbf{W}_{k+1} \mathbf{A}. \tag{56}$$

By substituting (55) and (56) into (54), we have

$$\mathbf{Q}_{\mathcal{I}_{k+P-1}} = [\mathbf{I} - \mathbf{G}_{\mathcal{I}_{K-1}} (\mathbf{G}_{\mathcal{I}_{K-1}}^H \mathbf{G}_{\mathcal{I}_{K-1}})^{-1} \mathbf{G}_{\mathcal{I}_{K-1}}^H] \times \mathbf{M}^T \mathbf{W}_{k+1} \mathbf{A} \mathbf{W}_{k+1}^H \mathbf{M}, \tag{57}$$

$$= \mathbf{P}_{\mathcal{I}_{K-2}} \mathbf{M}^T \mathbf{W}_{k+1} \mathbf{A} \mathbf{W}_{k+1}^H \mathbf{M}. \tag{58}$$

Thus, we arrive at:

$$\mathbf{P}_{\mathcal{I}_{k+P-1}} = \mathbf{I} - \mathbf{Q}_{\mathcal{I}_{k+P-1}}, \tag{59}$$

$$= \mathbf{I} - \mathbf{P}_{\mathcal{I}_{K-2}} \mathbf{M}^T \mathbf{W}_{k+1} (\mathbf{W}_{k+1}^H \mathbf{M} \mathbf{P}_{\mathcal{I}_{K-2}} \mathbf{M}^T \mathbf{W}_{k+1})^{-1} \times \mathbf{W}_{k+1}^H \mathbf{M}. \tag{60}$$

VII. Acknowledgements

The authors acknowledge the use of the IRIDIS High Performance Computing Facility, and associated support services at the University of Southampton, in the completion of this work.

References

[1] R. Mesleh, H. Haas, S. Sinanovic, C. Ahn and S. Yun "Spatial modulation," *IEEE Trans. Veh. Technol.*, vol. 57, no. 4, pp. 2228-2242, July 2008.

[2] M. Di Renzo, H. Haas and P. M. Grant, "Spatial modulation for multiple-antenna wireless systems - A Survey," *IEEE Commun. Magazine*, vol. 49, no. 12, pp. 182-191, Dec. 2011.

[3] M. Di Renzo, H. Haas, A. Ghrayeb, S. Sugiura and L. Hanzo, "Spatial modulation for generalized MIMO: challenges, opportunities, and implementation," *Proceedings of the IEEE*, vol. 102, no. 1, pp. 56-103, Jan. 2014.

[4] A. Stavridis, S. Sinanovic, M. Di Renzo and H. Haas, "Energy evaluation of spatial modulation at a multi-antenna base station," *2013 IEEE 78th Vehicular Technology Conference (VTC Fall)*, Las Vegas, NV, 2013.

[5] P. Som and A. Chockalingam, "Spatial modulation and space shift keying in single carrier communication," *IEEE 23rd International Symposium on Personal, Indoor and Mobile Radio Communications - (PIMRC)*, Sydney, NSW, pp. 1962-1967, 2012.

[6] R. Rajashekar, K.V.S. Hari and L. Hanzo, "Spatial modulation aided zero-padded single carrier transmission for dispersive channels," *IEEE Trans. Commun.*, vol. 61, no. 6, pp. 2318-2329, Jun. 2013.

[7] P. Yang *et al.*, "Single-carrier SM-MIMO: A promising design for broadband large-scale antenna systems," *IEEE Communications Surveys & Tutorials*, vol. 18, no. 3, pp. 1687-1716, Third quarter 2016.

[8] L. He, J. Wang and J. Song, "Information-aided iterative equalization: A novel approach for single-carrier spatial modulation in dispersive channels," *IEEE Trans. Veh. Technol.*, vol. 66, no. 5, pp. 4448-4452, May 2017.

[9] R. Rajashekar, K.V.S. Hari, L. Hanzo, "Reduced-complexity ML detection and capacity-optimized training for spatial modulation systems," *IEEE Trans. Commun.*, vol. 62, no. 1, pp. 112-125, Jan. 2014.

[10] P. Yang, M. Di Renzo, Y. Xiao, S. Li and L. Hanzo, "Design guidelines for spatial modulation," *IEEE Communications Surveys & Tutorials*, vol. 17, no. 1, pp. 6-26, First quarter 2015.

[11] N. Ishikawa, R. Rajashekar, S. Sugiura and L. Hanzo, "Generalized-spatial-modulation-based reduced-RF-chain millimeter-wave communications," *IEEE Trans. Veh. Technol.*, vol. 66, no. 1, pp. 879-883, Jan. 2017.

[12] P. Yang, Y. Xiao, Y. L. Guan, Z. Liu, S. Li and W. Xiang, "Adaptive SM-MIMO for mmWave communications with reduced RF chains," *IEEE J. Sel. Areas Commun.*. vol. 35, no. 7, pp. 1472-1485, Jul. 2017.

[13] P. Wolniansky, G. Foschini, G. Golden and R. Valenzuela, "V-BLAST: an architecture for realizing very high data rates over the rich-scattering wireless channel," *in Proc. International Symp. Signals, Syst., Electron.*, Pisa, Italy, pp. 295-300, Sep. 1998.

[14] V. Tarokh, N. Seshadri and A. R. Calderbank, "Space-time codes for high data rate wireless communication: performance criterion and code construction," *IEEE Trans. Inf. Theory*, vol. 44, no. 2, pp. 744-765, Mar. 1998.

[15] S. M. Alamouti, "A simple transmit diversity technique for wireless communications," *IEEE J. Sel. Areas Commun.*, vol. 16, no. 8, pp. 1451-1458, Oct. 1998.

[16] E. Basar, U. Aygolu, E. Panayirci and H. V. Poor, "Space-time block coding for spatial modulation," *IEEE Trans. Commun.*, vol. 59, no. 3, pp. 823-832, Mar. 2011.

[17] R. Rajashekar and K.V.S. Hari, "Modulation diversity for spatial modulation using complex interleaved orthogonal design," *in Proc. IEEE TENCON 2012*, pp. 1-6, Nov. 2012.

[18] X. Li and L. Wang, "High rate space-time block coded spatial modulation with cyclic structure," *IEEE Commun. Lett.*, vol. 18, no. 4, pp. 532-535, Apr. 2014

[19] A. G. Helmy, M. Di Renzo and N. Al-Dhahir, "Enhanced-reliability cyclic generalized spatial-and-temporal modulation," *IEEE Commun. Lett.*, vol. 20, no. 12, pp. 2374-2377, Dec. 2016.

[20] P. Yang, Y. Xiao, L. Li, Q. Tang, Y. Yu and S. Li, "Link adaptation for spatial modulation with limited feedback," *IEEE Trans. Veh. Technol.*, vol. 61, no. 8, pp. 3808-3813, Oct. 2012.

[21] R. Rajashekar, K.V.S. Hari and L. Hanzo, "Antenna selection in spatial modulation systems," *IEEE Commun. Lett.*, vol. 17, no. 3, pp. 521-524, Mar. 2013.

[22] R. Rajashekar, K.V.S. Hari, K. Giridhar and L. Hanzo, "Performance analysis of antenna selection algorithms in spatial modulation systems with imperfect CSIR," *European Wireless 2013; 19th European Wireless Conference*, Guildford, UK, pp. 1-5, 2013.

[23] Z. Zhou, N. Ge and X. Lin, "Reduced-complexity antenna selection schemes in spatial modulation," *IEEE Commun. Lett.*, vol. 18, no. 1, pp. 14-17, Jan. 2014.

[24] N. Wang, W. Liu, H. Men, M. Jin, and H. Xu, "Further complexity reduction using rotational symmetry for EDAS in spatial modulation," *IEEE Commun. Lett.*, vol. 18, no. 10, pp. 1835-1838, Oct. 2014.

[25] R. Rajashekar, K.V.S. Hari and L. Hanzo, "Quantifying the transmit diversity order of Euclidean distance based antenna selection in spatial modulation," *IEEE Signal Proc. Lett.*, vol. 22, no. 9, pp. 1434-1437, Sep. 2015.

[26] Z. Sun, Y. Xiao, L. You, L. Yin, P. Yang and S. Li, "Cross-entropy-based antenna selection for spatial modulation," *IEEE Commun. Lett.*, vol. 20, no. 3, pp. 622-625, Mar. 2016.

[27] P. Yang, Y. Xiao, Y. L. Guan, S. Li and L. Hanzo, "Transmit antenna selection for multiple-input multiple-output spatial modulation systems," *IEEE Trans. Commun.*, vol. 64, no. 5, pp. 2035-2048, May 2016.

[28] Z. Sun *et al.*, "Transmit antenna selection schemes for spatial modulation systems: search complexity reduction and large-scale MIMO applications," *IEEE Trans. Veh. Technol.*, vol. 66, no. 9, pp. 8010-8021, Sep. 2017.

[29] Y. Naresh and A. Chockalingam, "On media-based modulation using RF mirrors," *IEEE Trans. Veh. Technol.*, vol. 66, no. 6, pp. 4967-4983, Jun. 2017.

[30] R. Rajashekar, M. Di Renzo, K.V.S. Hari and L. Hanzo, "A generalised transmit and receive diversity condition for feedback assisted MIMO systems: Theory & applications in full-duplex spatial modulation," *IEEE Trans. Signal Proc.*, vol. 65, no. 24, pp. 6505-6519, Dec. 15, 2017.

[31] M. C. Lee, W. H. Chung and T. S. Lee, "Generalized precoder design formulation and iterative algorithm for spatial modulation in MIMO systems with CSIT," *IEEE Trans. Commun.*, vol. 63, no. 4, pp. 1230-1244, Apr. 2015.

[32] P. Yang, Y. L. Guan, Y. Xiao, M. D. Renzo, S. Li and L. Hanzo, "Transmit precoded spatial modulation: Maximizing the minimum Euclidean distance versus minimizing the bit error ratio," *IEEE Trans. Wireless Commun.*, vol. 15, no. 3, pp. 2054-2068, Mar. 2016.

[33] B. L. Hughes, "Differential space-time modulation," *IEEE Trans. Inform. Theory*, vol. 46, no. 7, pp. 2567-2578, Nov. 2000.

[34] Y. Bian, X. Cheng, M. Wen, L. Yang, H.V. Poor, and B. Jiao, "Differential spatial modulation," *IEEE Trans. Veh. Technol.*, vol. 64, no. 7, pp. 3262-3268, Jul. 2015.

[35] N. Ishikawa and S. Sugiura, "Unified differential spatial modulation," *IEEE Wireless Commun. Lett.*, vol. 3, no. 4, pp. 337-340, Aug. 2014.

[36] W. Zhang, Q. Yin, and H. Deng, "Differential full diversity spatial modulation and its performance analysis with two transmit antennas," *IEEE Commun. Lett.*, vol. 19, no. 4, pp. 677-680, Apr. 2015.
[37] R. Rajashekar, N. Ishikawa, S. Sugiura, K.V.S. Hari, and L. Hanzo, "Full-diversity dispersion matrices from algebraic field extensions for differential spatial modulation," *IEEE Trans. Veh. Technol.* vol. 66, no. 1, pp. 385-394, Jan. 2017.
[38] P. A. Martin, "Differential spatial modulation for APSK in time-varying fading channels," *IEEE Commun. Lett.*, vol. 19, no. 7, pp. 1261-1264, Jul. 2015.
[39] J. Liu, L. Dan, P. Yang, L. Xiao, F. Yu, and Y. Xiao, "High-rate APSK-aided differential spatial modulation: Design method and performance analysis," *IEEE Commun. Lett.*, vol. 21, no. 1, pp. 168-171, Jan. 2017.
[40] M. Wen, X. Cheng, Y. Bian, and H. V. Poor, "A low-complexity near-ML differential spatial modulation detector," *IEEE Signal Proc. Lett.*, vol. 22, no. 11, pp. 1834-1838, Nov. 2015.
[41] R. Rajashekar, C. Xu, N. Ishikawa, S. Sugiura, and L. Hanzo, "Algebraic differential spatial modulation is capable of approaching the performance of its coherent counterpart," *IEEE Trans. Commun.*, vol. 65, no. 10, pp. 4260-4273, Oct. 2017.
[42] M. Wen, X. Cheng, and L. Yang, "Index modulation for 5G wireless communications." New York, NY, USA: Springer, 2017.
[43] R. Rajashekar, K.V.S. Hari and L. Hanzo, "A reduced-complexity partial-interference-cancellation group decoder for STBCs," *IEEE Signal Proc. Lett.*, vol. 20, no. 10, pp. 929-932, Oct. 2013.
[44] G. H. Golub, "Matrix computations," *Johns Hopkins University*, 1983.
[45] D. Tse and P. Viswanath, "Fundamentals of wireless communication." *Cambridge University Press*, 2005.

Rakshith Rajashekar (M'14-SM'17) received the B.E. degree in electrical communication engineering from Visvesvaraya Technological University, Karnataka, India, in 2007. He received his Ph.D. from the Department of Electrical Communication Engineering, Indian Institute of Science (IISc), India, in 2014. He is presently working as a Research Fellow at the University of Southampton (UoS), UK. Before joining the UoS, he worked at Accord Software & Systems, Bengaluru, India, as a Systems Engineer from 2007 to 2009, and as a Senior Scientist at Broadcom Communications, Bengaluru, India from 2014 to 2015. His research interests include antenna selection in MIMO systems, differential communication, millimeter wave communication, communication between drones with a focus on space-time signal processing and coding. He is the recipient of the Special Recognition award from Broadcom Communications, India and the Dean's Award from the UoS, UK, for excellence in research. He has received the Best Reviewer award from IEEE Transactions on Wireless Communications and the Exemplary Reviewer award from IEEE Wireless Communications Letters.

K.V.S. Hari (M'92-SM'97-F'15) received the B.E. degree from Osmania University, Hyderabad, India, in 1983; the M.Tech. degree from the Indian Institute of Technology Delhi, New Delhi, India, in 1985; and the Ph.D. degree from the University of California at San Diego, La Jolla, CA, USA, in 1990.Since 1992, he has been with the Department of Electrical Communication Engineering, Indian Institute of Science, Bangalore, India, where he is currently a Professor and coordinates the activities of the Statistical Signal Processing Laboratory. He was an Affiliated Professor (2010-16) with the Department of Signal Processing, KTH Royal Institute of Technology, Stockholm, Sweden. He has been a Visiting Faculty Member with Stanford University, Stanford, CA, USA; KTH Royal Institute of Technology, Stockholm, Sweden; and Aalto University, Espoo, Finland (formerly Helsinki University of Technology). While at Stanford University, he worked on multiple-input multiple-output (MIMO) wireless channel modelling and co-authored the Worldwide Interoperability for Microwave Access standard on wireless channel models for fixed-broadband wireless communication systems, which proposed the Stanford University Interim channel models. He was also with the Defence Electronics Research Laboratory, Hyderabad, and the Research and Training Unit for Navigational Electronics, Osmania University. His research interests include the development of signal processing algorithms for MIMO wireless communication systems, sparse signal recovery problems, indoor positioning, assistive technologies for the elderly, and neuroscience. Dr. Hari was an Editor of Elsevier's EURASIP journal Signal Processing (2006-16) and the Senior Associate Editor of Springer's Indian Academy of Sciences journal SADHANA. He is an Academic Entrepreneur and a Cofounder of the company ESQUBE Communication Solutions, Bangalore. He received the Institution of Electronics and Telecommunication Engineers S. V. C. Aiya Award for Excellence in Telecom Education and the Distinguished Alumnus Award from the Osmania University College of Engineering, Hyderabad. He is a Fellow of the Indian NAE.

Lajos Hanzo (http://www-mobile.ecs.soton.ac.uk) FREng, FIEEE, FIET, Fellow of EURASIP, DSc received his degree in electronics in 1976 and his doctorate in 1983. In 2009 he was awarded an honorary doctorate by the Technical University of Budapest and in 2015 by the University of Edinburgh. In 2016 he was admitted to the Hungarian Academy of Science. During his 40-year career in telecommunications he has held various research and academic posts in Hungary, Germany and the UK. Since 1986 he has been with the School of Electronics and Computer Science, University of Southampton, UK, where he holds the chair in telecommunications. He has successfully supervised 111 PhD students, co-authored 18 John Wiley/IEEE Press books on mobile radio communications totalling in excess of 10 000 pages, published 1685 research contributions at IEEE Xplore, acted both as TPC and General Chair of IEEE conferences, presented keynote lectures and has been awarded a number of distinctions. Currently he is directing a 60-strong academic research team, working on a range of research projects in the field of wireless multimedia communications sponsored by industry, the Engineering and Physical Sciences Research Council (EPSRC) UK, the European Research Council's Advanced Fellow Grant and the Royal Society's Wolfson Research Merit Award. He is an enthusiastic supporter of industrial and academic liaison and he offers a range of industrial courses. He is also a Governor of the IEEE VTS. During 2008 - 2012 he was the Editor-in-Chief of the IEEE Press and a Chaired Professor also at Tsinghua University, Beijing. For further information on research in progress and associated publications please refer to http://www-mobile.ecs.soton.ac.uk Lajos has 30 000+ citations and an H-index of 68.